

5 RESULTS

5.1 Determination of the selenium content in the culture medium

The level of selenium in the culture medium was measured by atomic absorption spectrometry. The medium and different FBS charges were subjected to analysis. It is extremely important to have a controlled concentration of selenium in the culture medium because the synthesis of selenoproteins depends on the presence of this trace element. The selenium quantity found in the samples measured is listed in Table 4. In the medium without FBS (DMEM) the selenium content was below the detection limit. In the two FBS charges analysed there was a considerable difference in the selenium content. For these studies the FBS charge with the smaller selenium content was used in order to have the possibility of increasing the selenium concentration in the cell culture medium and to study the consequences of these changes. Using 10 % fetal bovine serum (FBS Biochrom 224B) resulted in a selenium concentration of the medium below 15 nM selenium. In all experiments the basal selenium levels in control conditions were <15 nM.

<i>SAMPLE</i>	<i>c (Se) [μg/l]</i>
DMEM (BV2-COS7)	below detection limit
FBS Biochrom 661A	10.7 ± 0.1
FBS Biochrom 224B	8.4 ± 0.4

Table 4 Determination of the selenium concentration in different cell media and FBS charges.

5.2 Effect of selenite on BV2 cell viability

The effect of selenium on cells is concentration-dependent. At low levels, selenium is an essential trace element inducing the expression of selenoproteins. Higher concentrations are toxic and lead to cell death. The tolerable levels differ among cell types (112). The cell viability was investigated to determine the threshold Se concentration above which Se reduced the cell viability in BV2 cells. BV2 were

cultured in DMEM medium supplemented with 10 % FBS (charge 224B Biochrom, Berlin, Germany) and 50 U/ml penicillin/streptomycin under standard culture conditions and treated with various concentrations of sodium selenite (Na_2SeO_3). The content of selenium in the culture medium and in the FBS charges was below 15 nM (see previous paragraph). To assess the cell viability, the MTT test was performed (see 4.3.1). Cells were plated at a density of 4000 to 6000 cells per well on 96-well plates. In order to compare the data from different experiments regarding the capacity of cells for peroxide detoxification, it is extremely important to plate the cells at the same cell density. Sixteen hours later, the cells were treated with the indicated concentration of selenium (added as sodium selenite Na_2SeO_3) for 24 hours at 37 °C in a 5 % CO_2 incubator and the cell viability was assayed. It was found that the treatment with sodium selenite decreased the viability of BV2 cells in a dose-dependent manner. Figure 6 shows that selenite concentrations up to the micromolar range were tolerated by microglia without any influence on the cell viability, whereas higher amounts of selenium led to cell death. 10 μM selenite reduced the cell viability by about 10 % of the control inducing cytotoxicity probably by oxidative stress, inhibition of DNA-synthesis and induction of apoptosis.

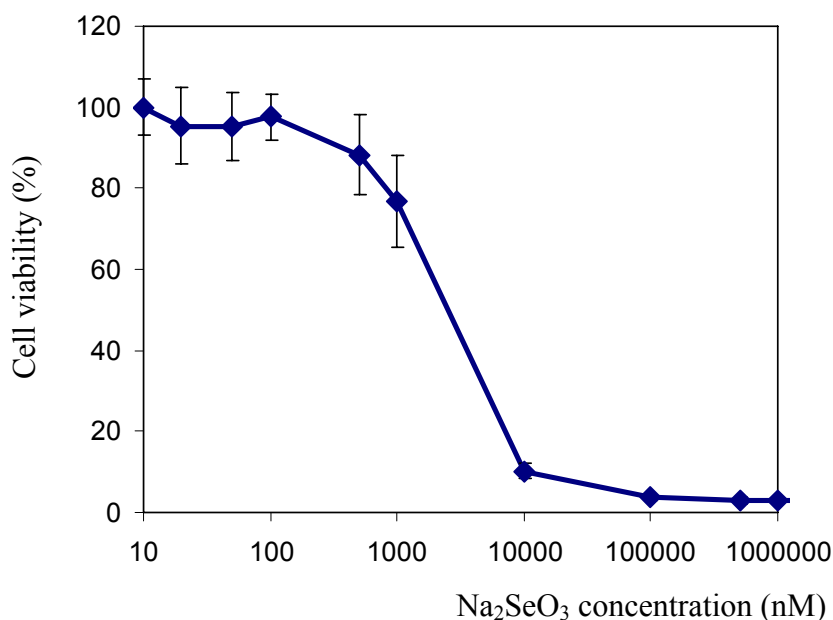


Figure 6 Concentration-dependent effect of selenium added as sodium selenite (Na_2SeO_3) on BV2 cell viability. Each point represents the mean \pm SD of 3 experiments.

5.3 Hydrogen peroxide toxicity in BV2 cells

Oxidative stress conditions were induced in BV2 by treatment with hydrogen peroxide (H_2O_2), that is toxic to cells and induces cell death in the brain. Hydrogen peroxide is a commonly used oxidant that passes freely through membranes and increases the intracellular level of peroxides, which thus could lead to cell death. Cells were treated for 12 hours with 250 μM hydrogen peroxide and the cell viability was determined by the MTT test as described in the method section. The exposure to H_2O_2 consistently produced a significant decrease in cell survival to values that were $< 20\%$ of those in control cells not exposed to H_2O_2 .

5.4 Selenium prevents H_2O_2 -mediated cell death

H_2O_2 treatment (as described above) reduced cell survival of BV2 cells. This H_2O_2 -induced cell death could be prevented by application of selenite in a concentration-dependent manner. Na_2SeO_3 was added to the cells one day before the H_2O_2 stress. After hydrogen peroxide supplementation, the cell viability was assessed. The data in Figure 7 are presented as % of the control (untreated cells). These data show that selenium, in the range between 0.030 and 1 μM protects microglial cells from H_2O_2 -induced cell death. This protective effect is not mediated directly by antioxidative effects of selenite but required probably de novo selenoprotein synthesis (113).

Taken into consideration the toxicity of selenite at levels above 10 μM in BV2 cells and the optimum protective level of 500 nM selenite against H_2O_2 treatment, a concentration of 500 nM sodium selenite was chosen in the following experiments.

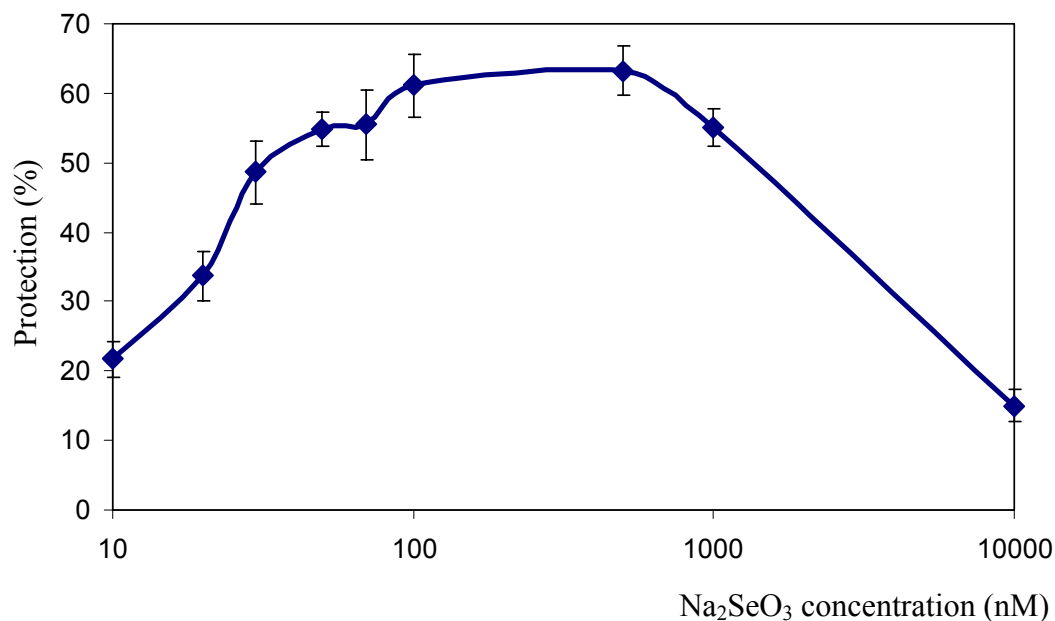


Figure 7 Concentration-dependent protection of selenium in H₂O₂ treatment. Selenite (Na₂SeO₃) was applied at different concentrations to the BV2 cells with subsequent addition of 250 μM H₂O₂ for 12 hours. The degree of protection was calculated as percentage of cell viability related to the control.

5.5 Selenium treatment reduces stress-induced migration of microglia

Microglial cells are activated by treatment with H₂O₂. Activated microglial are characterized by an amoeboid morphology, which is associated with an enhanced phagocytotic activity, up-regulation of various immuno-effector molecules, and the production of inflammatory and cytotoxic factors (114). For the migration assay, BV2 cells were plated at $2 \times 10^4/\text{cm}^2$ on a 2-well chamber slide (Nunc) and treated with 500 nM selenite. After 16 h incubation, 250 μM H₂O₂ was added and after the indicated time the cells were observed under a light microscope and counted. Cells treated with H₂O₂ showed a dramatic decrease of the cell number after 8 hours. This effect was almost completely inhibited by pre-treatment with selenite. H₂O₂ transforms microglial cells from a resting ramified form into an activated amoeboid form. This morphological change was prevented by selenite supplementation. The amoeboid-like

phenotype as well as the migratory activity could be reduced by selenite application within the physiological range (Figure 8).

This is an indication that the application of selenite inhibits the activation of microglial cells, which may contribute to the damage of neurons or other cell types in diseases characterized by an imbalance in the redox homeostasis.

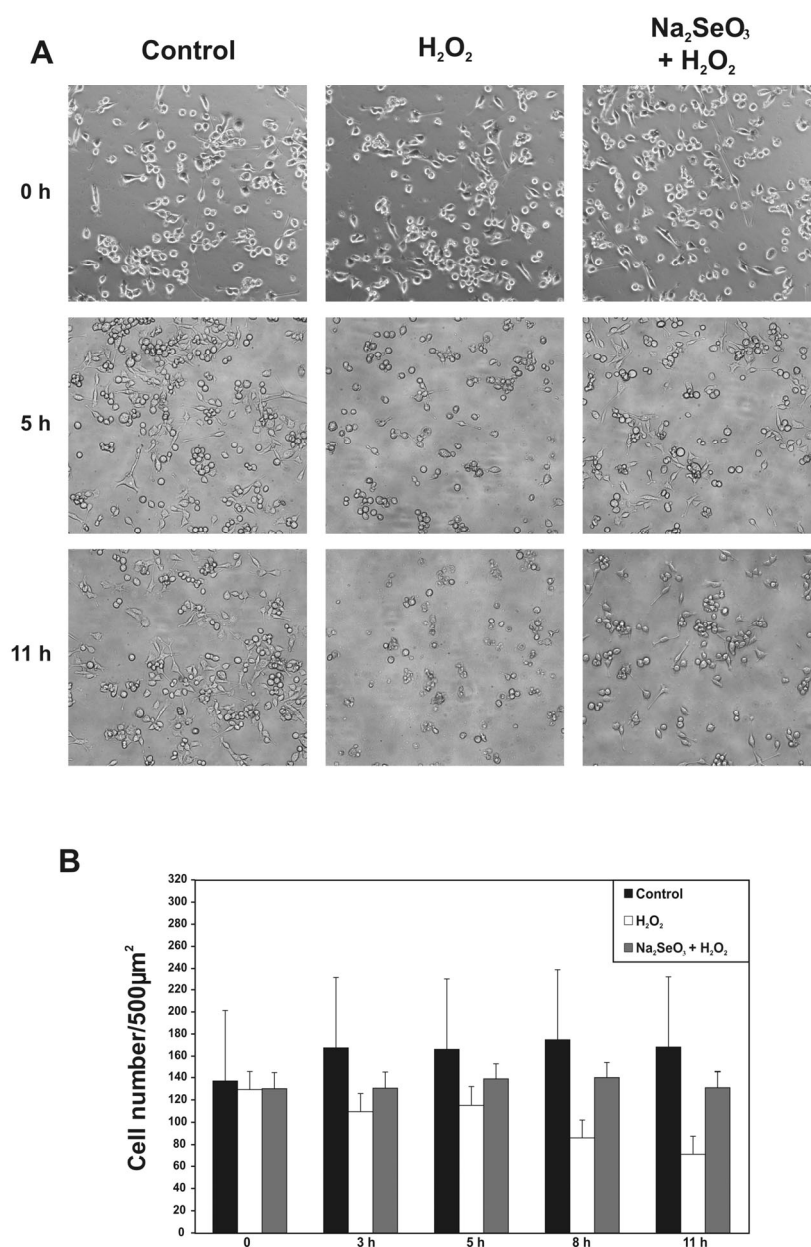


Figure 8 Migration assay. A) BV2 cells under a light microscope. Control: untreated cells. H₂O₂: cells incubated with 250 μM H₂O₂ for the indicated time. Na₂SeO₃ + H₂O₂: cells incubated with 500 nM selenite for 12 hours and with 250 μM H₂O₂ for the indicated time. B) Statistical quantification (mean ± SD) by counting: cells were counted by five independent investigators in a blind test.

5.6 Effect of selenium on adhesion molecule expression

The activation of microglial cells occurs during the pathogenesis of various neurologic diseases. Activated microglia show an up-regulation of integrins. Integrins comprise a large family of cell adhesion molecules that mediate interactions between the extracellular environment and the cytoplasm. They regulate many aspects of cell behaviour including survival, proliferation, migration and differentiation. The integrins are transmembrane receptors that consist of noncovalently bound heterodimers composed of α and β chains.

The expression of the surface integrin subunits CD11a (LFA-1 α chain) on BV2 cells was quantified by flow cytometry (FACS analysis). The cells were either unstimulated or activated by hydrogen peroxide. As shown in Figure 9, the expression of CD11a was upregulated after H_2O_2 treatment. The pretreatment with sodium selenite reduced the H_2O_2 -induced microglial activation.

The influence of selenite on the modulation of the adhesion molecule expression indicates a role of selenium in the immune response of microglia.

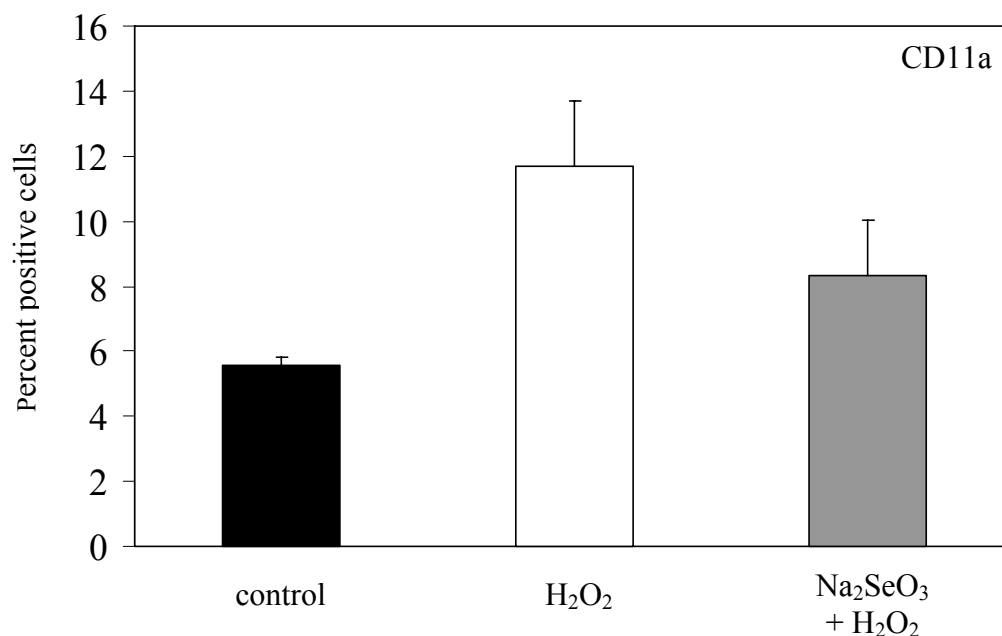


Figure 9 FACS analysis of CD11a expression in BV2 cells after pre-incubation with 500 nM selenium (selenite, Na_2SeO_3) and stimulation with 250 μM hydrogen peroxide (H_2O_2). Data are given as percent of positive cells \pm SD, $n=2$.

5.7 Selenium prevents H₂O₂-induced cell death and inhibits ROS generation

Hydrogen peroxide has been shown to increase the cellular oxidative stress. The exposure of microglial cultures to 250 μ M H₂O₂ for 12 hours decreased the percentage of living cells determined with the MTT assay, and consequently the total cell number in the cultures decreased progressively. This H₂O₂-induced cell death could be prevented by application of selenite, as shown in Figure 10 (A) in a concentration-dependent manner. In Figure 10 (B) pictures of BV2 cells after selenium/H₂O₂ treatment and addition of MTT are shown. The reduction of MTT in isolated cells is regarded as an indicator of cell redox activity. The reaction is attributed mainly to mitochondrial enzymes and electron carriers, thus cells with active mitochondria transform MTT into blue formazone crystals which are clearly visible.

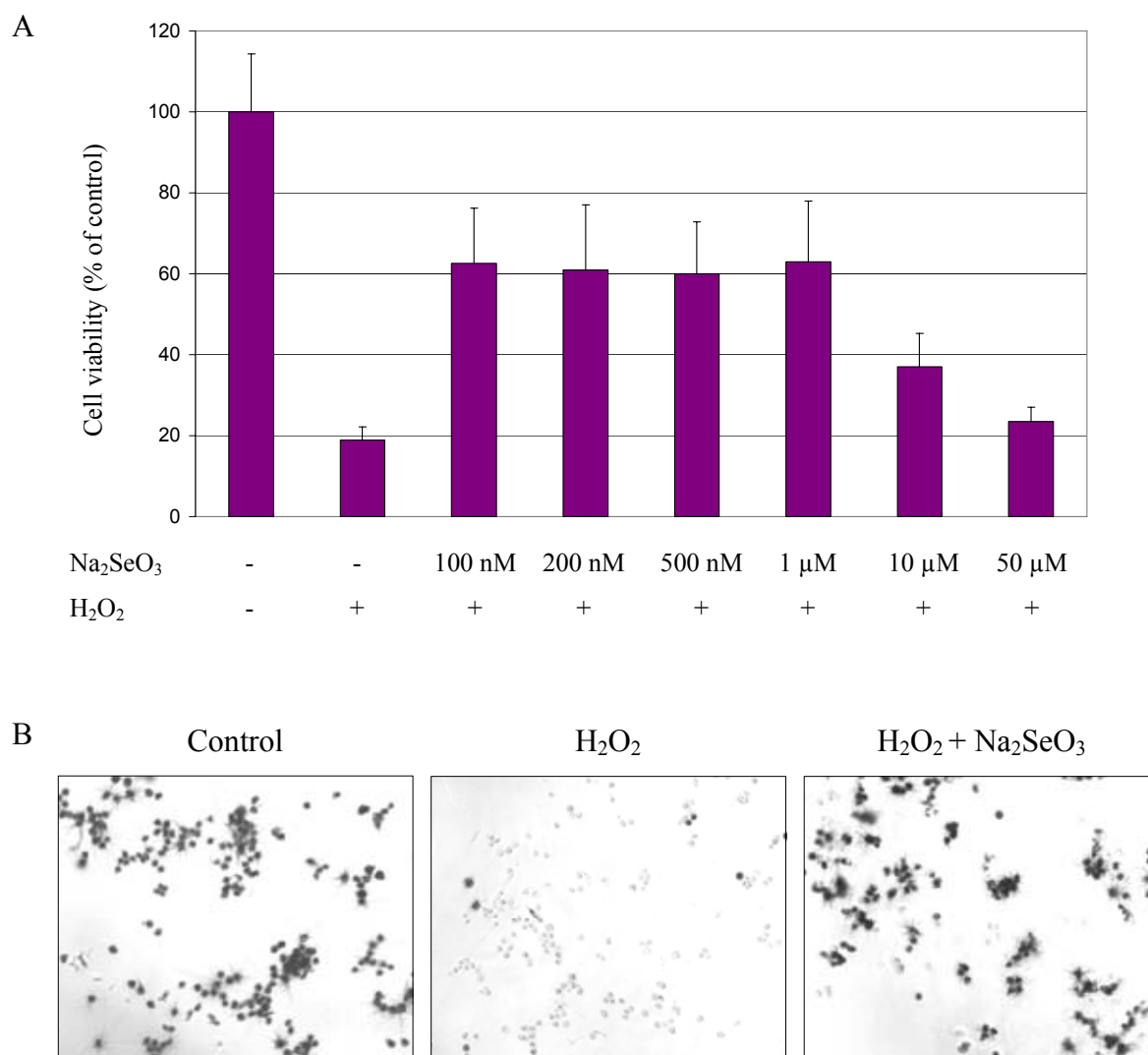


Figure 10 A) Concentration-dependent protective effects of selenium on BV2 cells treated with hydrogen peroxide. Sodium selenite (Na₂SeO₃) was applied at different concentrations to cells with subsequent addition of H₂O₂ (250 μM) and the cell viability was assayed with MTT (3-(4,5-Dimethylthiazol-2-yl)-2,5 diphenyltetrazolium bromide). B) BV2 cells investigated by light microscopy after addition of MTT. Control: untreated cells. H₂O₂: cells incubated with 250 μM H₂O₂. H₂O₂ + Na₂SeO₃: cells incubated with 500 nM selenite for 16 h and then with 250 μM H₂O₂.

Free oxygen radicals were monitored as a means to determine the degree of overall oxidative stress. The oxidation of nonfluorescent 2',7'-dichlorofluorescein (DCFH-DA) to a fluorescent product is currently used to evaluate oxidative stress in cells. This leads to an increased fluorescence and permits visualization of the relative levels of ROS.

DCFH-DA permeates living cells and is deacetylated by nonspecific intracellular esterases. In the presence of ROS, which are produced throughout the cell,

particularly during oxidative stress, the reduced fluorescein compound is oxidized and emits bright green fluorescence, which can be detected by a fluoroplate reader.

In BV2 cells the ROS levels rose after H₂O₂ treatment by a factor of 2.5 (Figure 11), but selenite pre-treatment (with 100 nM) drastically decrease the H₂O₂-induced ROS production.

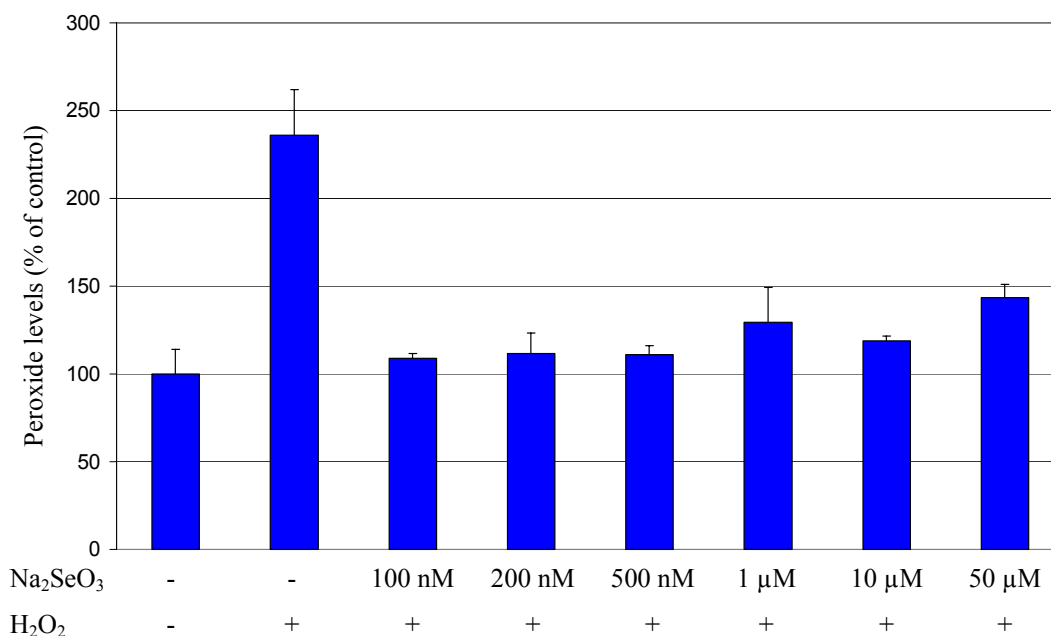


Figure 11 Concentration-dependent ROS inhibition by selenium in BV2 cells treated with hydrogen peroxide. Sodium selenite (Na₂SeO₃) was applied at different concentrations to cells with subsequent addition of H₂O₂ (250 μM) and the ROS were then measured.

These data show that physiological selenite concentrations protect microglial cells against H₂O₂-induced cell death and ROS generation during microglia activation. This finding suggests an important role of selenium in the prevention of oxidative stress involved in neurodegenerative diseases.

5.8 Studies on the activation of NF- κ B and iNOS

5.8.1 NF- κ B

NF- κ B is a member of a novel family of transcription factors sharing a common structural motif for DNA binding and dimerization. The DNA-binding, nuclear form of NF- κ B is composed of a heterodimer with a 50 kDa (p50) and a 65 kDa (p65) polypeptide. NF- κ B can rapidly activate the expression of genes involved in inflammatory, immune and acute phase response. Its activity is controlled by inhibitory subunits, called I κ B. I κ B is required for the inducible activation of NF- κ B. In non-stimulated cells, NF- κ B is not in the nucleus (and therefore does not activate genes) but in the cytoplasm, due to its association with I κ B (115). NF- κ B can be activated by many stimuli, such as hydrogen peroxide. To study the effect of selenite on the activation of NF- κ B, BV2 cells were incubated with H₂O₂ to initiate the NF- κ B activation cascade. One dish of BV2 was left untreated, one was pre-incubated with selenite followed by H₂O₂ treatment and one was treated with H₂O₂ for 12 hours. Nuclear extracts were prepared from these cells and assayed for NF- κ B expression by immunoblotting. Extracts with 25 μ g of proteins were separated on a 12.5 % SDS-polyacrylamide gel, transferred onto a nitrocellulose membrane and then analysed with an antibody against the NF- κ B subunit p65. The specific binding of the first antibody was detected by counterstaining with a horseradish peroxidase-linked antibody and visualized by the ECL-detection kit.

Figure 12 shows the Western blot of nuclear proteins in BV2 cells for NF- κ B and its evaluation. The nuclear expression of the NF- κ B subunit p65 was consistently increased after exposure to H₂O₂. In BV2 cells preincubated with 500 nM selenite, the peroxide-induced increase in the NF- κ B protein level did not occur.

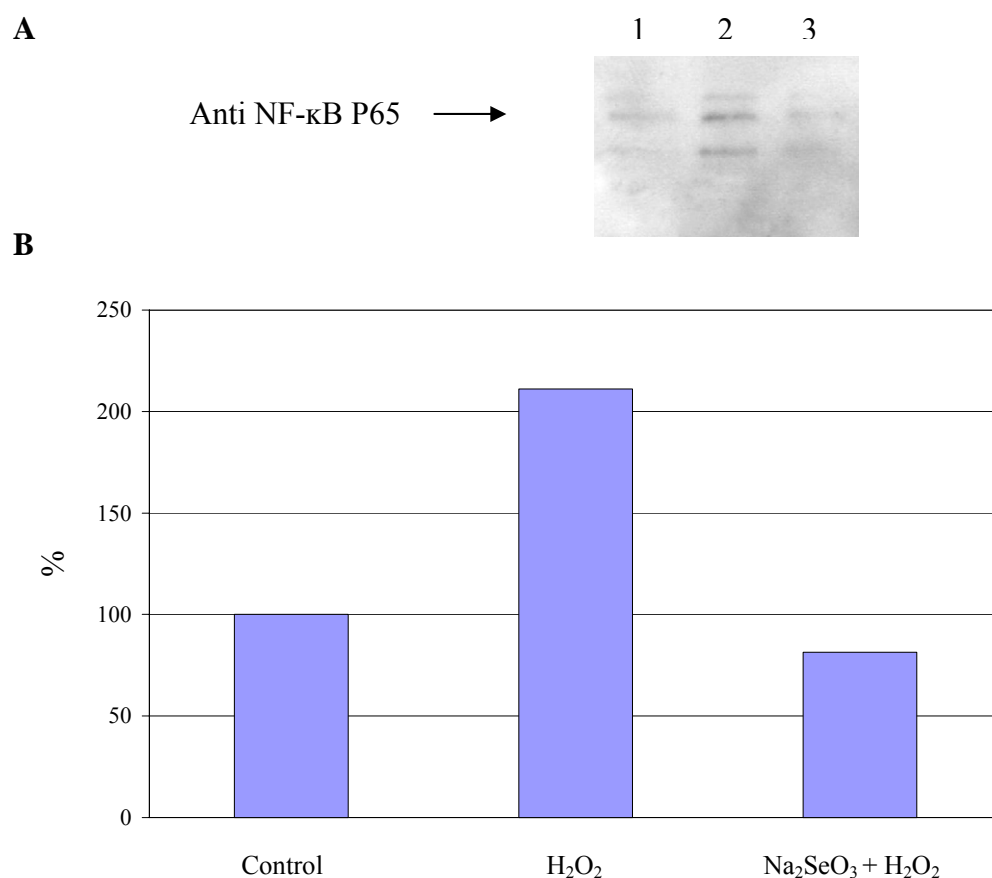


Figure 12 Inhibition of NF- κ B activation by selenite A) Western blot analysis with protein extracts from the nuclear extract of BV2 cells without treatment (lane 1), with 250 μ M H₂O₂ treatment for 4 hours (lane 2) or with preincubation with 500 nM Na₂SeO₃ (lane 3). B) Quantitative evaluation of the Western blot by densitometry (control set as 100 %).

5.8.2 iNOS

Inducible nitric oxide synthase (iNOS) is associated with microglia in neurodegenerative diseases (116). Glia activation involves changes in cell phenotype and gene expression, including activation of the inducible isoform of nitric oxide synthase (iNOS). It is discussed in the literature that activated glia can kill neurons in coculture (117-119), and this can occur in vivo during brain trauma, inflammation, ischemia, post-infection and in neurodegenerative diseases (120). Because the iNOS gene is expressed predominantly by microglia, studies have focused on factors regulating iNOS expression.

To investigate iNOS expression and its regulation by H_2O_2 and to determine if selenium interferes, a Western blot of BV2 cytoplasmic proteins was performed. A significant increase of iNOS expression was observed in BV2 cells 24 h after H_2O_2 addition (Figure 13). The Western blots showed the significant prevention of iNOS expression after selenite pre-treatment. Selenite suppressed the H_2O_2 -induced inducible nitric oxide synthase (iNOS) gene transcription. Because iNOS is responsible for the release of the toxic free radical NO that leads to neurodegenerative processes, the inhibitory effect of selenite could be advantageous to counteract secondary neuronal cell death.

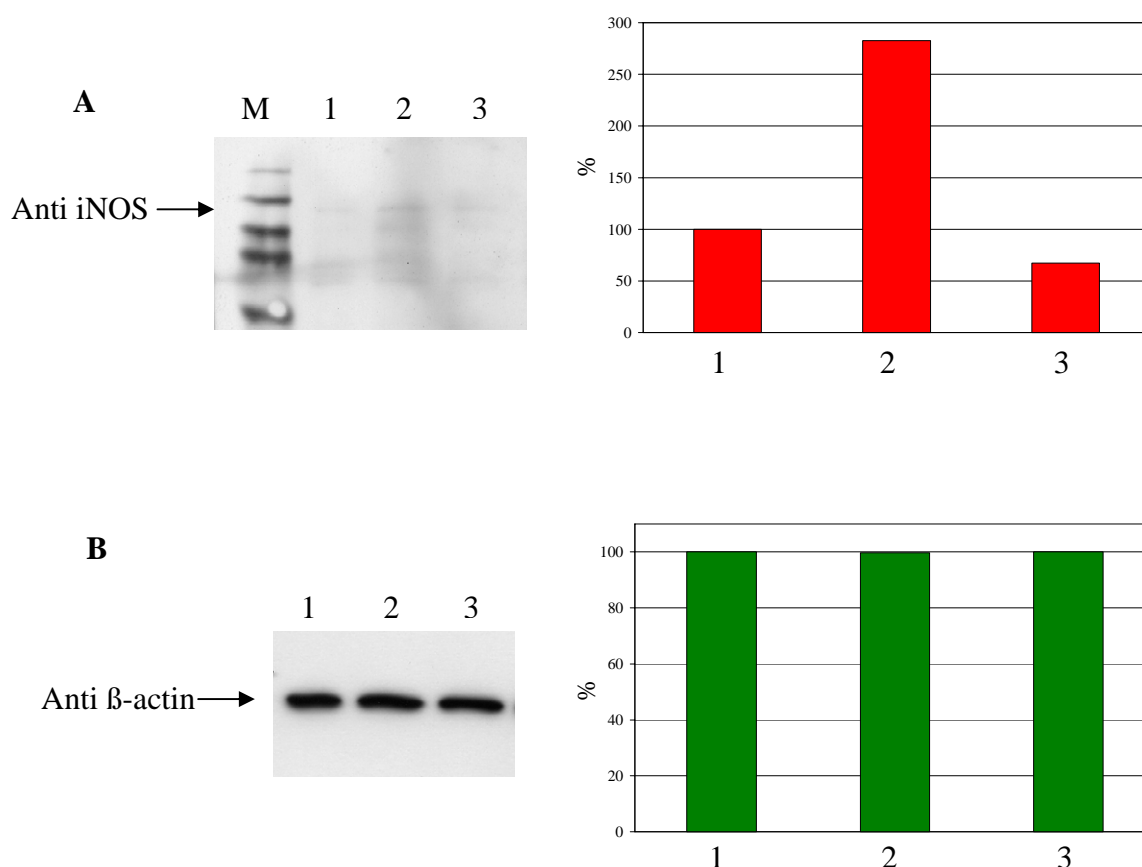


Figure 13 iNOS Western blotting. A) Western blot representation and quantification of iNOS expression in BV2 cytoplasm of cells untreated (lane 1, control), treated with H_2O_2 (lane 2, H_2O_2) and preincubated with selenite (lane 3, $H_2O_2 + Na_2SeO_3$). B) Western blot representation and quantification of β -actin expression in the same samples, which demonstrates an equal loading of proteins. Control set at 100 %.

5.9 Analysis of apoptosis

In order to assess the effects of selenium supplementation on the protection against apoptotic cell death, apoptosis was evaluated by several methods in BV2 cells subjected to oxidative stress.

5.9.1 Selenium and CASPASE-3

Diverse groups of molecules are involved in the apoptosis pathway. One set of mediators implicated in apoptosis belong to the aspartate-specific cysteinyl proteases or caspases. A member of this family, caspase-3 (CPP32) has been identified as a key mediator of apoptosis of mammalian cells. Caspase-3 exists in cells as an inactive 32 kDa proenzyme, called pro-caspase-3. Pro-caspase-3 is cleaved into active 17 and 12 kDa subunits by upstream proteases such as caspase 6 and caspase 8 during apoptosis. Untreated BV2 (control), BV2 treated with selenite, H₂O₂ or selenite + H₂O₂ were lysed and ~ 10 µg of protein were separated on an SDS gel and transferred to a nitrocellulose membrane. The membrane was incubated overnight with 5 % dry skim milk to block non-specific binding. Then it was incubated with rabbit anti-Caspase-3 (1:1000) for 2 hours at room temperature. Subsequently, the membrane was incubated with a conjugated goat anti-rabbit IgG. The caspase-3 protein was detected by a chemiluminescence detection system (ECL) and scanned. Equal loading of protein was checked by β-actin immunoblotting indicated by a 42 kDa band on the membrane.

Figure 14 shows that H₂O₂ induced the activation of caspase-3. Selenite alone had no effect. The treatment with selenite was shown to inhibit the hydrogen peroxide-induced activation of proteases (caspase-3). This result clearly shows that the application of selenite at the indicated concentration was able to prevent the cascade of caspase activation.

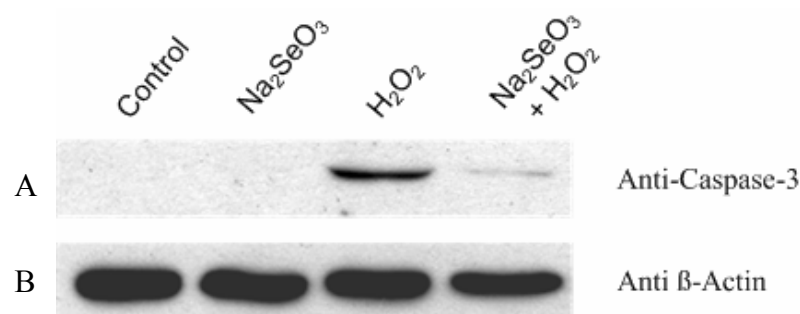


Figure 14 Western blot of the whole cell extract of microglial cells (BV2) separated on SDS-PAGE and blotted with polyclonal anti-caspase-3 (A) and monoclonal anti-β-actin (load control) (B). Control: untreated cells. Na₂SeO₃: application of 500 nM sodium selenite. H₂O₂: application of 250 μM hydrogen peroxide. Na₂SeO₃ + H₂O₂: pre-treatment with 500 nM sodium selenite and subsequent application of hydrogen peroxide.

5.9.2 Selenium and ANNEXIN V

Apoptosis is a form of programmed cell death that is characterized by a variety of morphological features. In the early stages of apoptosis, changes occur at the cell surface. One of these plasma membrane alterations is the translocation of phosphatidylserine (PS) from the inner side of the plasma membrane to the outer layer, by which PS becomes exposed at the external surface of the cell (121).

The analysis of phosphatidylserine on the outer leaflet of apoptotic cell-membranes was performed by using Annexin V-FITC staining by FACS (Fluorescence Activated Cell Sorter). Annexin V is a Ca²⁺-dependent phospholipid-binding protein that has a high affinity for PS, and binds to cells with exposed PS.

Apoptosis in BV2 cells was induced by incubation with 250 μM H₂O₂ for 4 hours. BV2 cells were also pretreated with 500 nM sodium selenite (Na₂SeO₃) for 16 hours. Forward scatter (FSC)- side scatter (SSC) plots of BV2 cells show well-defined cell populations (Figure 15). In the FSC-SSC plots, FSC, a measure of cell size, is plotted against SSC, a measure of granularity. A gate from the population of viable cells was manually selected on the basis of their characteristic forward and side light-scattering, and the events were shown in a FL-1 (FITC) versus FL-2 plot.

As shown in Figure 15, untreated cells were primarily Annexin V-FITC negative, indicating that they were viable and not undergoing apoptosis. After a 4 hour-

treatment with 250 μM H_2O_2 , about 40 % of the cells were undergoing apoptosis (Annexin V-FITC positive). Preincubation with sodium selenite inhibited the apoptosis. The amount of apoptotic cells were then about 14 %, comparable to untreated cells that showed about 9 % Annexin V positive cells.

In Figure 16 a graph shows the effect of selenite supplementation on the exposure of PS recognised by Annexin-V staining.

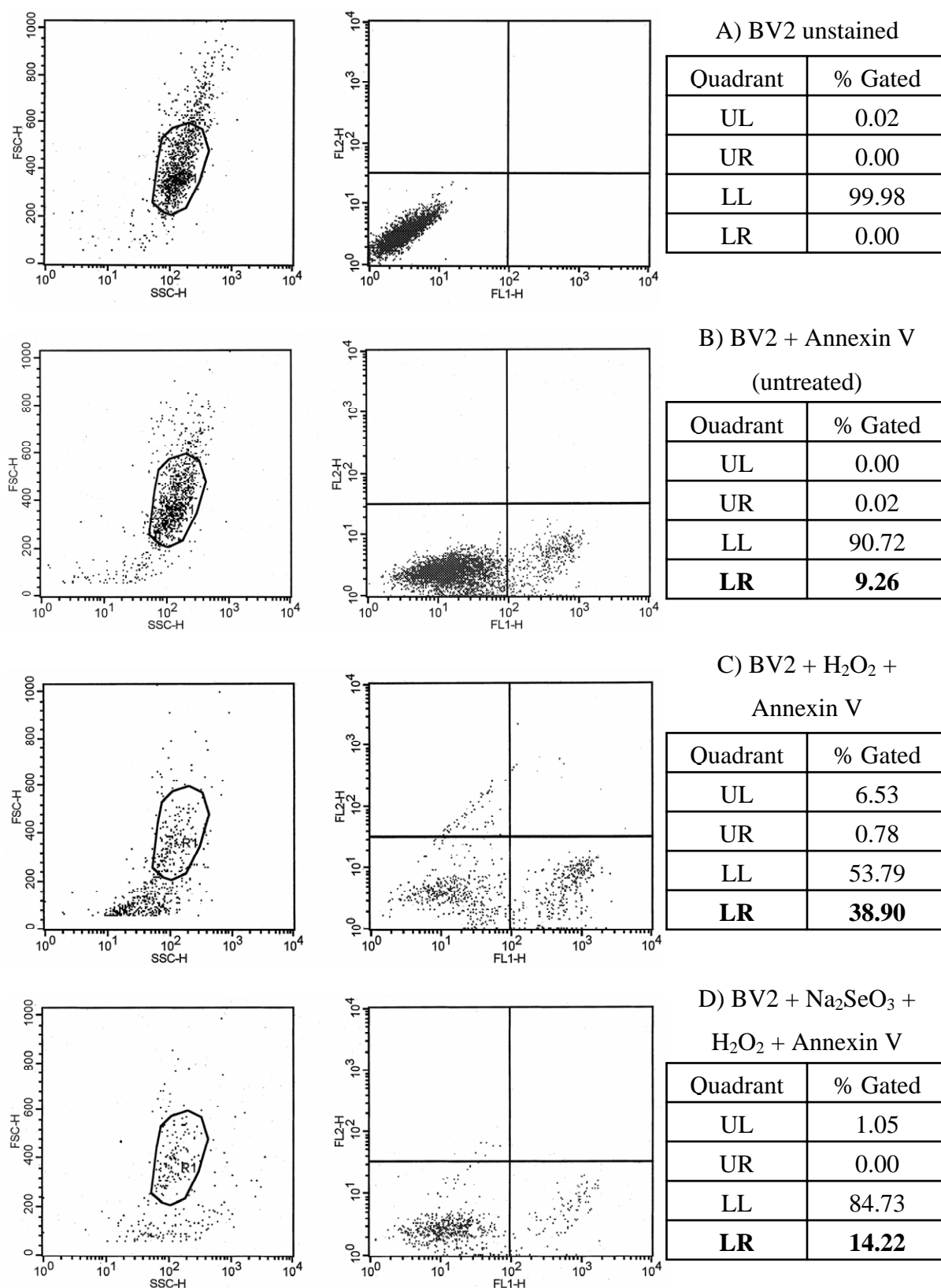


Figure 15 Analysis of the H₂O₂-mediated apoptosis in BV2 cells by Annexin V-FITC staining. Left: FSC-SSC plots of BV2 cells. Right: Contour diagram of Annexin V-FITC cytometry of BV2 cells (FL1-H: signal for Annexin V-FITC). BV2 were manually gated (R1) on the basis of their characteristic forward and light-scattering properties. The lower left quadrants (LL) of each panel show the viable cells, which are negative for Annexin V-FITC binding. The lower right (LR) quadrants represent the apoptotic cells (positive for Annexin V-FITC). One representative experiment is shown.

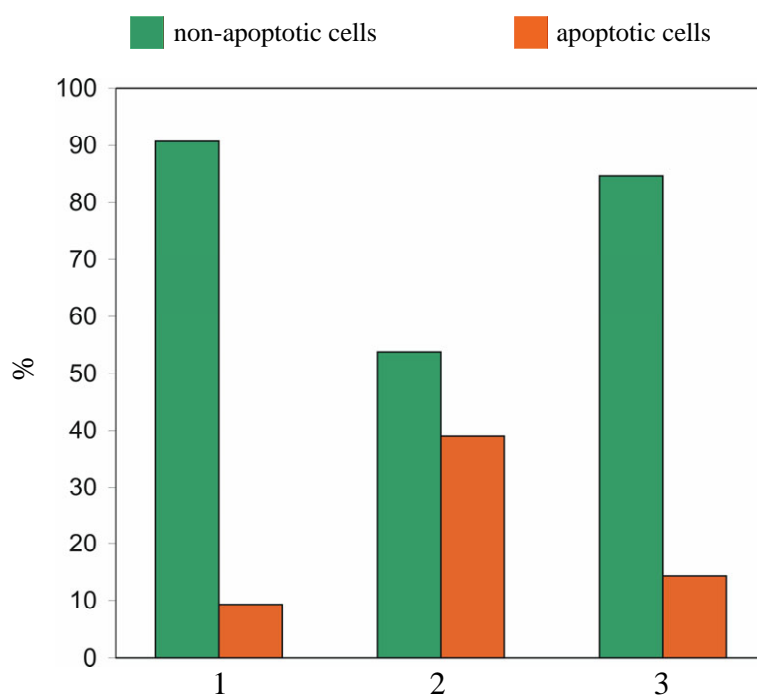


Figure 16 Apoptosis in BV2 cells. Quantification of non-apoptotic and apoptotic cells after treatment: 1- BV2-control stained with Annexin V-FITC; 2- BV2- H₂O₂ stained with Annexin V-FITC; 3- BV2- Na₂SeO₃ + H₂O₂ stained with Annexin V-FITC. Data were obtained from the experiment shown in Figure 15 (non-apoptotic cells LL, apoptotic cells LR).

These data suggest that selenium reduces the induced exposure of phosphatidylserine to the outer side of the cell membrane, that means it prevents the induction of apoptosis in its early stages.

5.10 Incorporation of ^{75}Se into BV2 cells

5.10.1 The selenoproteome of BV2 cells

The pattern of selenoproteins (selenoproteome) in BV2 cells was obtained by 2D PAGE after labelling of the cells with ^{75}Se -selenite. Labelling cells with ^{75}Se -selenite is a sensitive method for assessing the expression of selenoproteins. The combination of two-dimensional electrophoresis and ^{75}Se -labelling allowed an overview on the selenoproteins present in the sample.

BV2 cells were seeded on 10-cm dishes at 1×10^6 cells/dish and treated with 2 kBq/ml of ^{75}Se -selenite in 10 ml of culture medium (corresponding to about 0.027 nM Se). Since the equilibration process of exogenous ^{75}Se -selenite with the endogenous pool of Se and selenoproteins may need 24 hours, such labelling experiments require incubation with ^{75}Se for 48-36 hours.

The cells were allowed to grow for 48 hours at 37 °C in 5 % CO_2 and were then harvested and homogenized as previously described. An aliquot of total protein (500 μg) was separated by two-dimensional (2D) electrophoresis. The gels were silver-stained, dried and then exposed to a photostimulable phosphor-plate for 5 days. The Fuji BAS1000 system with AIDA software from Raytest was used for the recording of the autoradiogram.

Figure 17 and Figure 18 show the silver-stained 2D-gel and the autoradiogram, respectively.

In the one-dimensional SDS-PAGE (on the left side of the gel, Figure 18) six major ^{75}Se -labelled selenoproteins were observed, with mean molecular masses of about 10, 15, 20, 25, 60 and 65 kDa. In the autoradiogram of the 2D-gel, the labelled bands found after one-dimensional SDS-PAGE were resolved into more than 25 selenium-containing spots with molecular masses between 6 and 80 kDa and isoelectric points in the range between 3 and 10.

The selenoproteome of BV2 cells is not yet known and systematic studies on distinct selenoproteins in microglial cells are still lacking. In this work the different selenoproteins expressed in microglial cells have been classified for the first time. Some selenoproteins were identified by comparison with the results of previous studies on different cells lines with respect to their molecular masses and their pI

(Table 5). Selenoprotein P (SelP) is an extracellular heparin-binding glycoprotein that contains 10-17 selenocysteine residues per polypeptide. Four isoforms of the protein have been identified in rat plasma, including the full-length protein containing all 10 selenocysteines, and three shortened isoforms terminating in the parts of the sequence where the second, third, and seventh selenocysteine residue was predicted to be. For that reason, several spots on the 2D-gel could be attributed to the different SelP isoforms.

Thioredoxin reductase (TrxR) activity was also detected in the brain in previous studies. Three distinct thioredoxin reductases are identified, however, several splice variants are also known to exist. TrxR1 (ubiquitous cytoplasmatic enzyme) and TrxR2 (mitochondrial) were detected in the BV2 selenoproteome, indicating the presence of an effective antioxidative system in the microglial cells.

The deiodinases cleave specific iodine-carbon bonds in thyroid hormones, thereby regulating their hormonal activity. The brain takes up thyroxine (T₄) from the blood and converts it locally to T₃ so that it is not dependent on the systemic T₃ production in liver, kidney and thyroid. The T₃ production in the brain is necessary, as there is very little absorption of bloodstream T₃ across the blood-brain barrier to enter the central nervous system (122). Most of the 5' deiodinase present in the brain is attributed to the type 2 deiodinase, DI2 and to DI3 (123). Both, DI2 and also DI3 were detected in the microglial selenoproteome.

The family of glutathione peroxidases include several isoenzymes that play an important role in the body's antioxidative armoury. In the 2D-autoradiography of BV2, Gpx1 Gpx3 and Gpx4 were detected as spots with molecular masses of about 25, 23 and 20 respectively.

The 15 kDa selenoprotein was first detected in ⁷⁵Se-labelling studies in the prostate (124) with a pI-value of about 4.5 on the 2D-gel. The same spot was found in the BV2 cells. Speculations on its functions indicate a role of this protein in cancer prevention and cancer development.

Some other moderately ⁷⁵Se-labelled selenoproteins were most probably SelO, SPS2 and Sel M. A number of weakly labelled selenoproteins were also observed. However, more studies are required to obtain more detailed information on the complete selenoproteome of microglial cells.

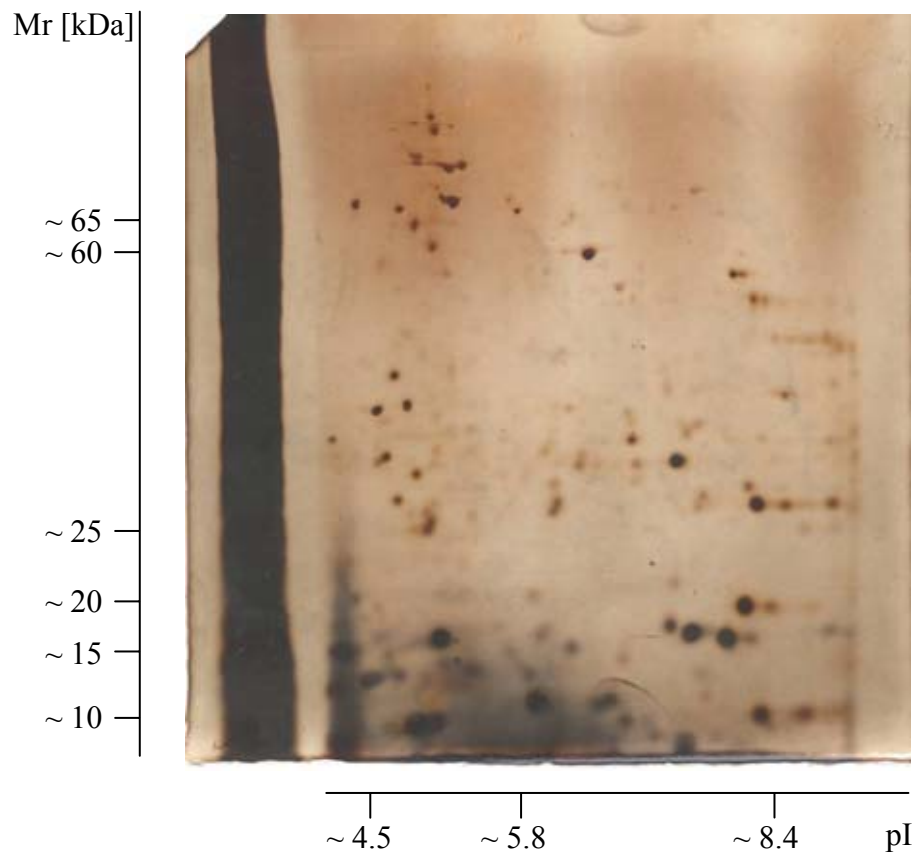


Figure 17 Two-dimensional electrophoresis pattern of BV2 lysate. Silver-stained gel. 500 μ g proteins were used for isoelectric focusing with immobilized pH linear gradient strips, pH range 3–10. In the second dimension the proteins were resolved by SDS-PAGE on 12 % polyacrylamide gels.

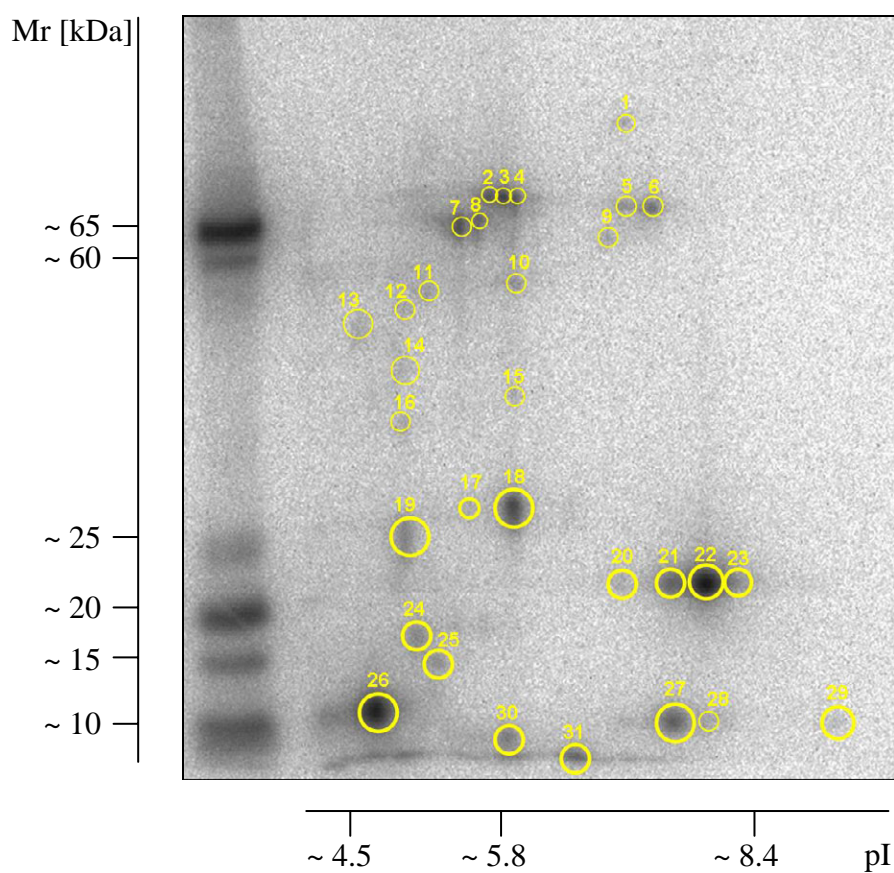


Figure 18 Microglial selenoproteome. Autoradiogram of the 2D-gel shown in Figure 17. The selenoproteins are marked in yellow (see text and **Table 5** for details).

SPOT	SELENOPROTEIN NAME
1	SelO ?
2-4	SelP ?
5-6	SPS2 ?
7-8	TrxR
9	?
10	DI3 ?
11-14	?
15	DI2 ?
16	?
17-18	Gpx1
19	?
20-23	Gpx4
24	SelM ?
25	?

26	15 kDa
27	15 kDa
28	?
29	SelW
30	?
31	SelR ?

Table 5 List of selenoproteins in microglial BV2 cells. The protein spot numbers correspond to those indicated in Figure 18.

5.10.2 Selenoprotein expression in BV2 in response to sodium selenite.

To examine the effect of selenium supplementation on the selenoprotein expression, BV2 cells were cultured in 75-cm² flasks supplemented with ⁷⁵Se-selenite (2 kBq/ml) with 30 to 500 nM sodium selenite added as carrier. After 36 hours, the proteins were extracted and 200 µg were subjected to one dimensional SDS-PAGE. The selenoproteins were visualized by autoradiography. The upper part (A) of Figure 19 shows the autoradiogram with the labelled selenoproteins and the lower part (B) its evaluation, that is the quantification of the relative intensity of each labelled protein band.

As described briefly in the previous paragraph, the most intensely labelled selenoproteins in BV2 cells were in the molecular mass range of about 65, 60, 25, 20, 15 and 10 kDa. The pattern of the labelled selenoproteins did not change after increasing the sodium selenite concentration in the culture medium. The general decrease in the activity in the sample (from control to addition of 500 nM Na₂SeO₃, lane 1 to 6 Figure 19 A) was due to the lower specific activity of ⁷⁵Se after addition of the inactive selenium carrier.

The supplementation with selenium affected the synthesis of specific selenoproteins. There was an increase in the relative intensity of the bands in the range of about 25 and 10 kDa.

Higher but still non-toxic concentrations of selenite (500 nM) resulted in a 5-fold increase in the 25 kDa band intensity (protein level) in the BV2 cells as compared with controls. This band was identified as the subunit of the glutathione peroxidase 1

enzyme (Gpx1). The result showed that there was a notable increase in the Gpx1 protein expression after selenium supplementation.

The band at about 10 kDa could include the selenoprotein W (SelW). The decrease of this protein in Se-deficient animals was originally reported as one of the factors of white muscle disease. SelW was expressed also in the brain, and its expression level was increased in response to the selenium supplementation (125). Its function is not yet clear, but it might possibly have an antioxidant function.

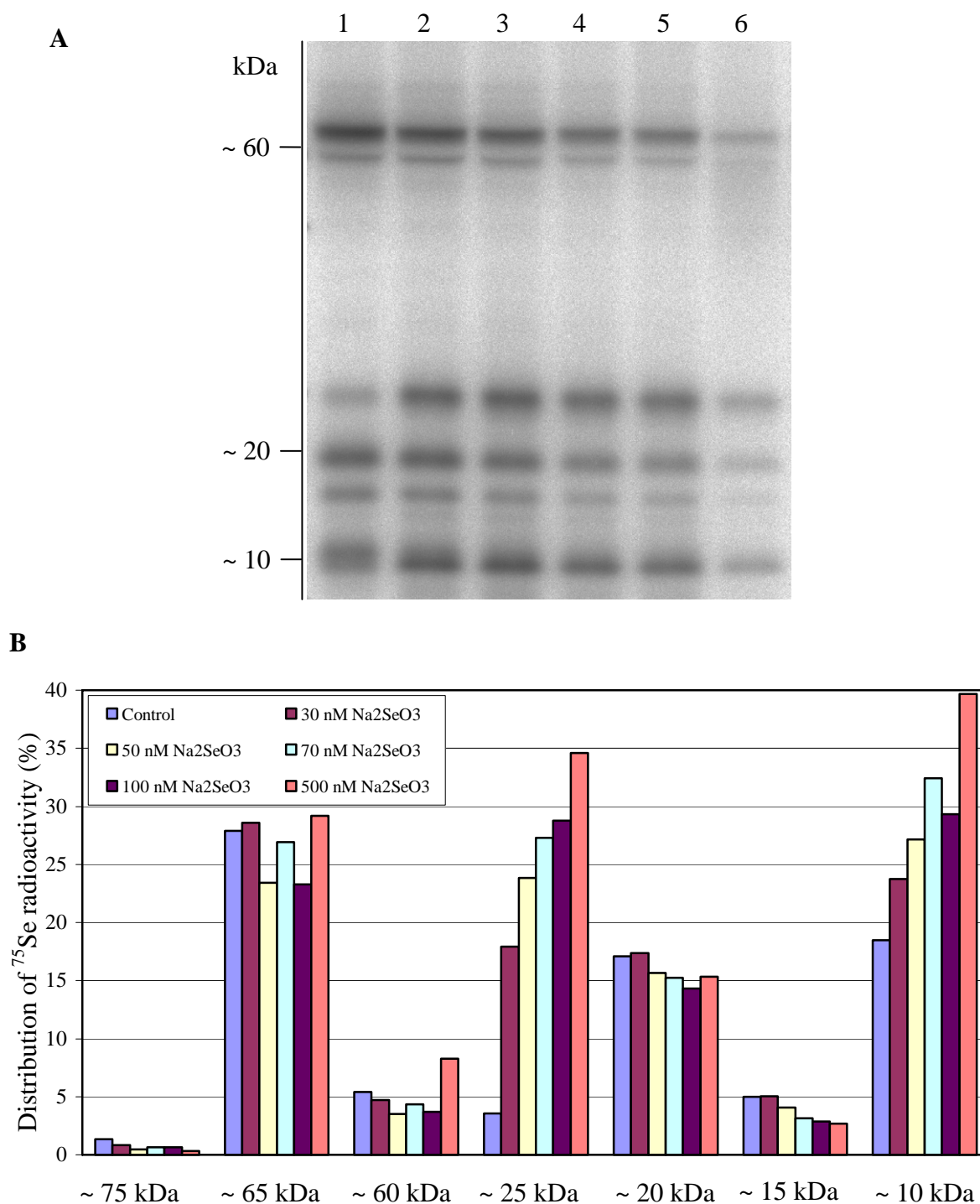


Figure 19 Analysis of BV2 selenoproteins after Se (sodium selenite, Na₂SeO₃) supplementation. Total protein extracts of BV2 cells, incubated with different amounts of selenite and with 20 kBq ⁷⁵Se-selenite for 36 hours, were subjected to SDS-PAGE and autoradiography. A) Autoradiogram of the labelled proteins. Lane 1: control, BV2 treated only with 20 kBq ⁷⁵Se. Lane 2: addition of 30 nM selenite. Lane 3: addition of 50 nM selenite. Lane 4: addition of 70 nM selenite. Lane 5: addition of 100 nM selenite. Lane 6: addition of 500 nM selenite. B) The distribution of radioactive ⁷⁵Se among the protein bands in the gel after SDS-PAGE (evaluation by means of the AIDA software) expressed as % of the total ⁷⁵Se activity in the lane.

Figure 20 shows in detail the selenoprotein distribution after 30 nM selenite supplementation and in the non-supplemented-control.

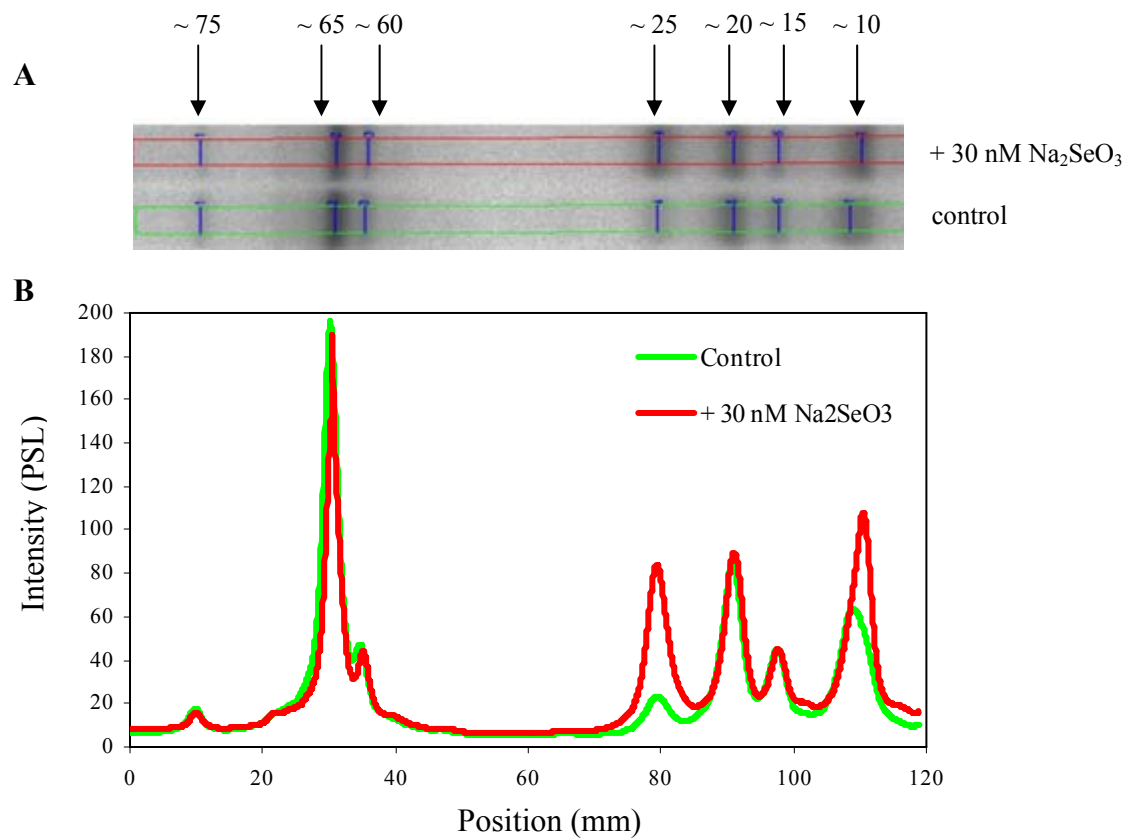


Figure 20 A) Autoradiogram of a gel after SDS-PAGE showing the ⁷⁵Se-selenite labelled selenoproteins in the total protein extract of BV2 cells. B) Evaluation of the autoradiogram shown in A using the Advanced Image Data Analyzer software (AIDA from Raytest).

5.11 Effect of selenite on the expression of selected selenoprotein

It has been shown that in all cultures the supplementation with sodium selenite had an effect on the expression of selenoproteins (see previous paragraph). In order to identify in more detail which specific selenoenzymes were up-regulated, a series of Western blots and enzyme activity assays was performed.

5.11.1 Western blot SelP and TrxR1

Because of the importance of the Trx system and SelP for many aspects of cell functions, the TrxR1 and SelP protein levels were investigated. TrxR1 is an enzyme belonging to the flavoprotein family of pyridine nucleotide-disulphide oxidoreductase. TrxRs are named for their ability to reduce oxidized thioredoxins (Trxs), a group of small ubiquitous redox-active peptides (126).

Selenoprotein P is an abundant extracellular glycoprotein that is rich in selenocysteine. Its concentration in plasma depends on the nutritional selenium intake of the individual, making it a useful biomarker of the selenium status. It functions in the distribution of selenium from the liver to the peripheral tissues such as the brain. There is also evidence for its function as an antioxidant, protecting cells from oxidant molecules (20).

Selenoprotein P (SelP) and thioredoxin reductase 1 (TrxR1) expressions after selenium supplementation were assessed by immunoblot in microglia BV2 cells (Figure 21). The same blot was also tested for β -actin protein to assure the equal protein loading. SelP and TrxR1 expression was not significantly changed after supplementation with 100 and 500 nM selenite. These data are consistent with the preceding experiment with ^{75}Se showing that the expression of some selenoproteins is not highly responsive to an increase in available selenium.

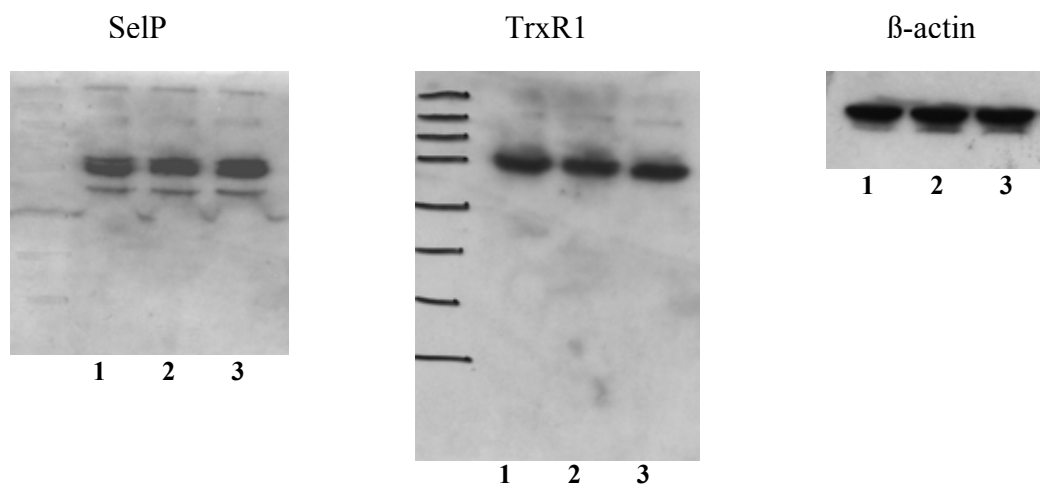


Figure 21 Analysis of SelP and TrxR1 expression. Immunoblots of SelP and TrxR1 in BV2 lysate (20 μ g pro lane). β -actin immunoblot is shown as protein loading control. The samples are as follows: lane 1, BV2 left untreated (control); lane 2, BV2 supplemented with 100 nM selenite for 24 hours; lane 3, BV2 supplemented with 500 nM selenite.

5.11.2 Effect of selenite on the cellular Gpx1 activity

In contrast to SelP and TrxR1, the results of the ^{75}Se experiment strongly suggest that the expression of a protein with an apparent molecular mass of about 25 kDa (Gpx1) was strongly increased after selenium supplementation. This suggested that the protective effect of selenite against H_2O_2 toxicity was due to the increase in the activity of this enzyme. To confirm this hypothesis, the Gpx1 enzyme activity was measured. The investigations of the Gpx1 activity were performed after incubation of cells with 100 and 500 nM selenite for 24 h.

The result presented in Figure 22 shows that the selenium treatment resulted in significant increases in the enzyme activity 24 h after supplementation. The treatment of the BV2 cells with 100 nM selenite increased the enzyme activity by about a factor of 3.5. Cells incubated with 500 nM selenite exhibited a 3.7-fold higher activity than the control (basal selenium < 15 nM). This result corresponds to the observation that preincubated BV2 cells are more resistant to toxic peroxide treatment as described previously. It is therefore most likely that the Gpx1 selenoenzyme is responsible for the protective effect of selenite in BV2 microglial cells.

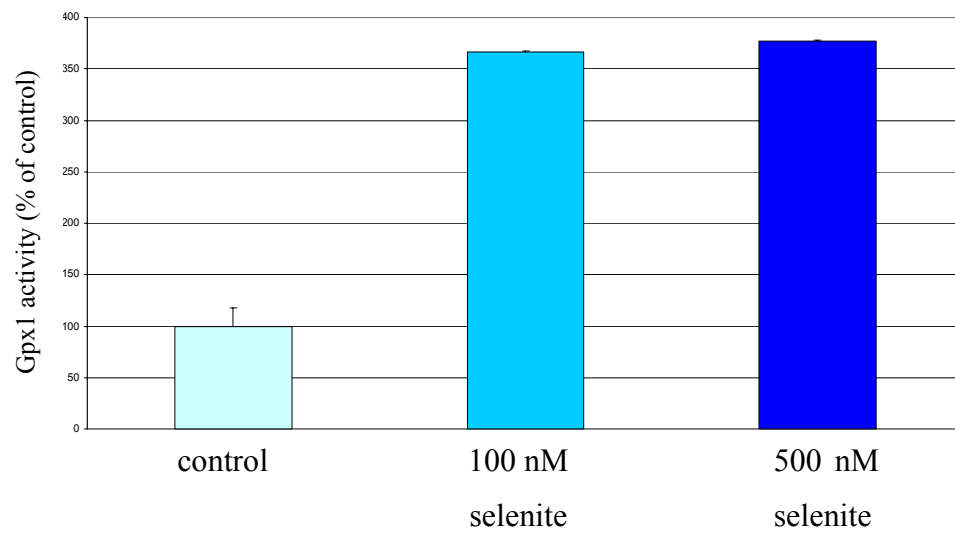


Figure 22 The effects of sodium selenite on Gpx1 in protein extracts from BV2 cells. The cells were grown for 24 h in the culture medium without or with addition of 100 and 500 nM sodium selenite. The data represent the mean of three experiments. Error bars represent the standard deviation.

5.12 Studies on BV2 cells treated with LPS - IFN γ

There are various microglial activators used in cells cultures. Two of them, interferon γ (IFN γ) and lipopolysaccharide (LPS), are named the conventional or orthodox activators (82). LPS and IFN γ have been used experimentally in combination or alone to induce nitric oxide (NO) production in microglial cells. Previous investigations have shown that the induction of iNOS mRNA and the consequent NO generation by LPS or IFN γ may be mediated by independent pathways (127). However, the exact intracellular signal pathways of microglial activation by LPS and IFN γ have not yet been clearly defined.

LPS is a glycolipid derived from the membrane surface of gram-negative bacteria (endotoxin), IFN γ is a cytokine produced by T-cells and natural killer cells in response to brain damage or disease states.

After LPS and IFN γ stimulation, microglia change their cellular functions radically, producing various types of inflammatory cytokines. They also induce NO production by stimulation of iNOS. The following sections will describe some experiments conducted on BV2 cells. First, information on the optimum of microglia activation was obtained by treatment of BV2 cells with different concentrations and different stimulation periods. Then the effect of selenium in these processes was investigated.

5.12.1 Cell viability of BV2 cells after LPS and IFN γ treatment

The cell viability was measured by means of the MTT test after incubation of the BV2 cells with different amounts of LPS (range 0.1 to 100 μ g/ml) and IFN γ (range 10 to 50 U/ml) for 48 hours (Figure 23). The MTT assay reflects the metabolic activity of cells and serves as a helpful indicator of cell viability.

LPS and IFN γ induce the death of BV2 cells in a dose-dependent manner. After a 48-hour incubation with 10 μ g/ml LPS, about 70 % of the cells survived. The rest was detached from the culture plates. By treatment with IFN γ (50 U/ml), about 60 % of BV2 cells died. These activator concentrations were used in the next experiment to test the possible involvement of selenite in these pathways.

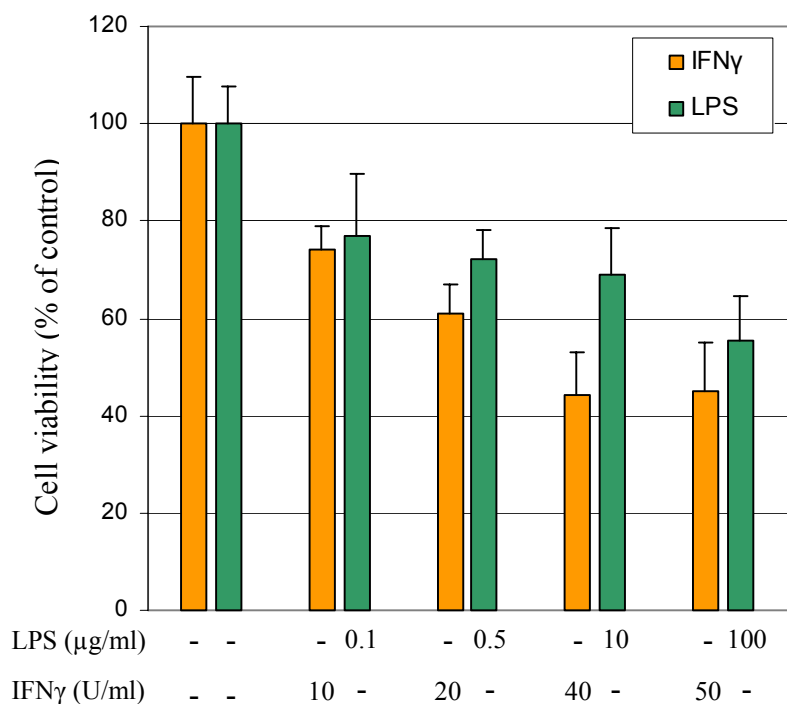


Figure 23 Effect of various concentrations of LPS and IFN γ on BV2 cell viability, measured by means of the MTT assay after a 48-hour incubation.

In order to examine the effect of selenium on the cell death induced by LPS and IFN γ , BV2 cells were pre-treated with 500 nM sodium selenite for one day prior to the stimulation with LPS (10 µg/ml) or IFN γ (50 U/ml) for up to 72 hours.

From the data shown in Figure 24 it could be concluded that selenite did not affect BV2 cell survival after LPS and IFN γ treatment.

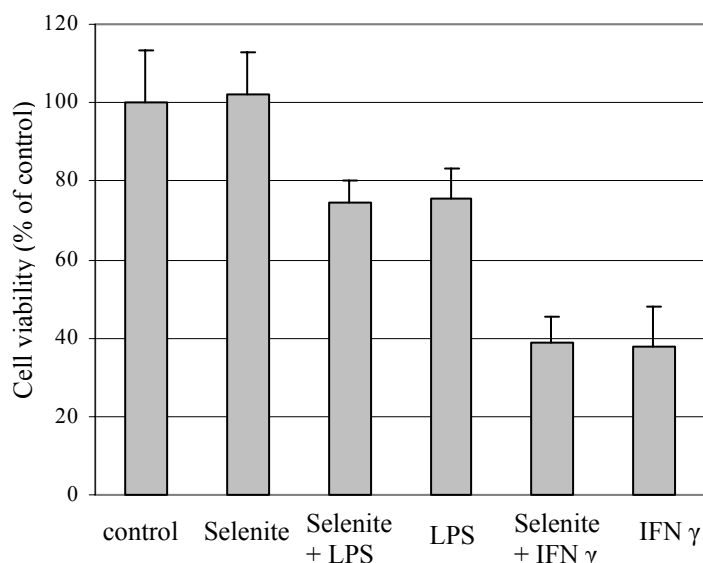


Figure 24 Effect of pre-treatment with selenite on BV2 cell viability. 500 nM Na₂SeO₃ was added 24 hours before LPS (10 μ g/ml) and IFN γ (50 U/ml) stimulation (48 hours).

5.12.2 NO production in BV2 cells after LPS and IFN γ stimulation

Activated microglia are thought to be involved in neuronal inflammation by over-producing various bioactive molecules such as nitric oxide (NO) (128).

In order to elucidate if selenium interferes with the LPS or IFN γ microglia activation pathways, experiments on the NO production were conducted.

The production of NO was assessed as the accumulation of nitrite in the medium using a colorimetric reaction with the Griess reagent as described in the method section.

LPS and IFN γ induced NO in BV2 in a time- and dose-dependent manner. Figure 25 confirmed that IFN γ is one of the most potent NO inducers in microglial cells. Its application (50 U/ml) for 48 hours increased the production of NO by factor of 160 as compared with the unstimulated cells. The treatment with LPS also increased the NO expression, as is extensively described in literature.

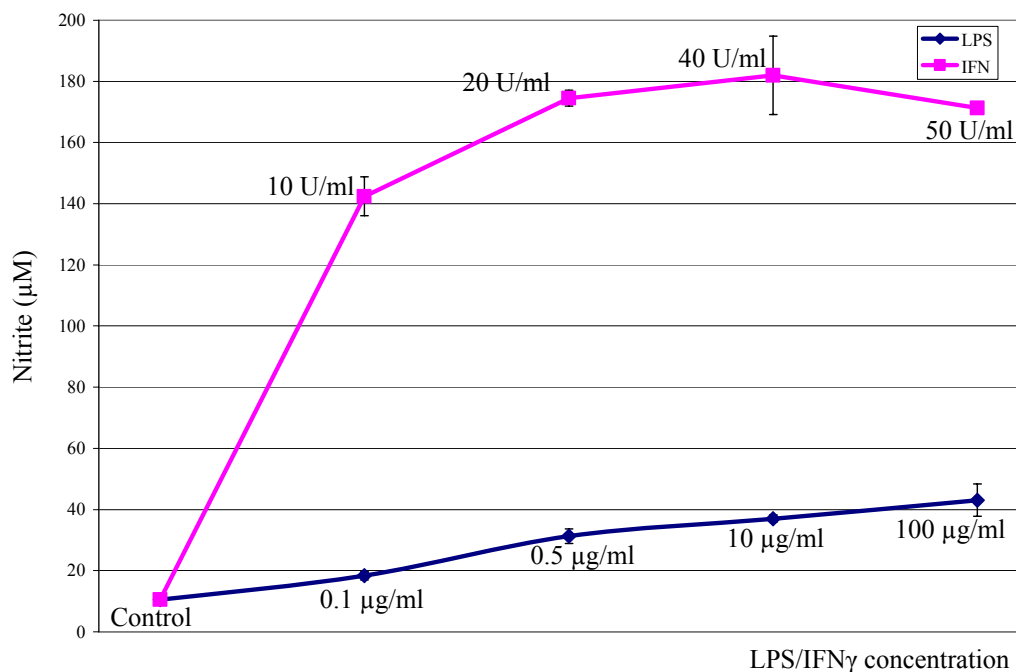


Figure 25 NO production in BV2 cells after a 48 hour stimulation with the indicated concentrations of LPS and IFN γ (determined by Griess assay, using sodium nitrite diluted to concentrations between 10-100 μ M to generate a standard curve).

Using cultured BV2 cells, the NO release by IFN γ was examined. After IFN γ treatment (from 10 to 50 U/ml), a significant amount of NO was detected after 24 hours and the release increased during the next hours (Figure 26).

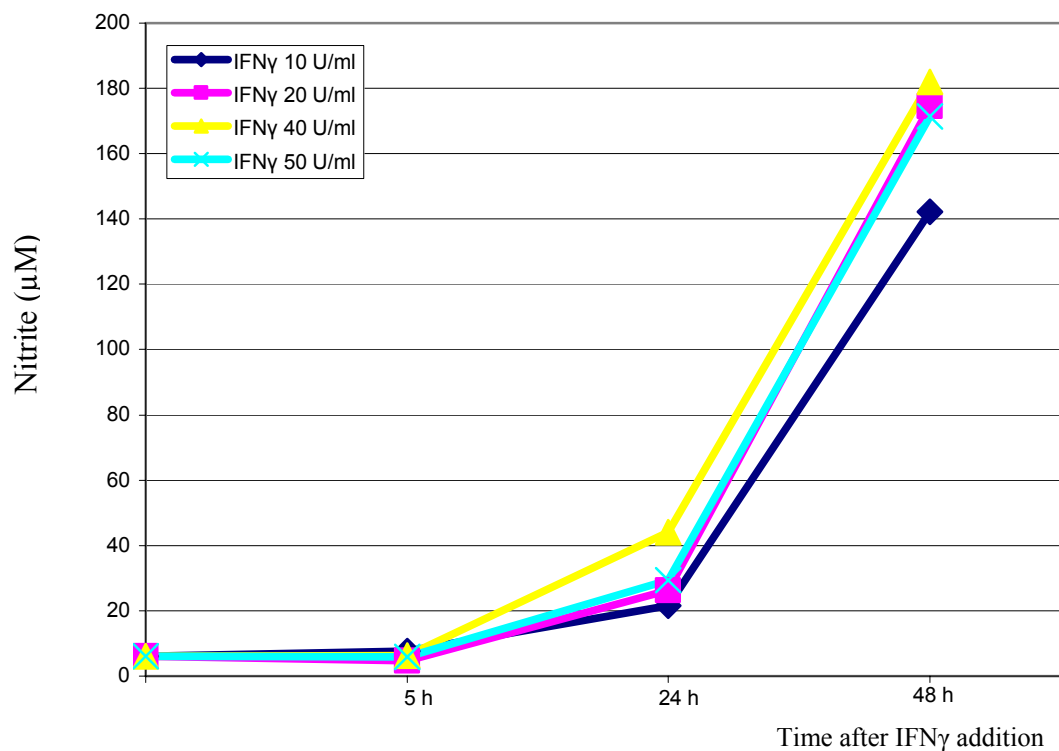


Figure 26 Time course of NO release induced by IFN γ from BV2 cells. At appropriate time points after addition of 10, 20, 40 and 50 U/ml IFN γ , NO production was determined by measuring nitrite, a stable oxidation product of NO, by the Griess method.

As these data on the production of nitric oxide confirmed the strong activation of microglial cells, 24 and 48 hours were chosen for the stimulation of BV2 cells with LPS and IFN γ .

When BV2 cells were preincubated with selenite (500 nM) for 24 hours and subsequently stimulated with LPS and IFN γ , no decreasing effect on NO production was observed (Figure 27).

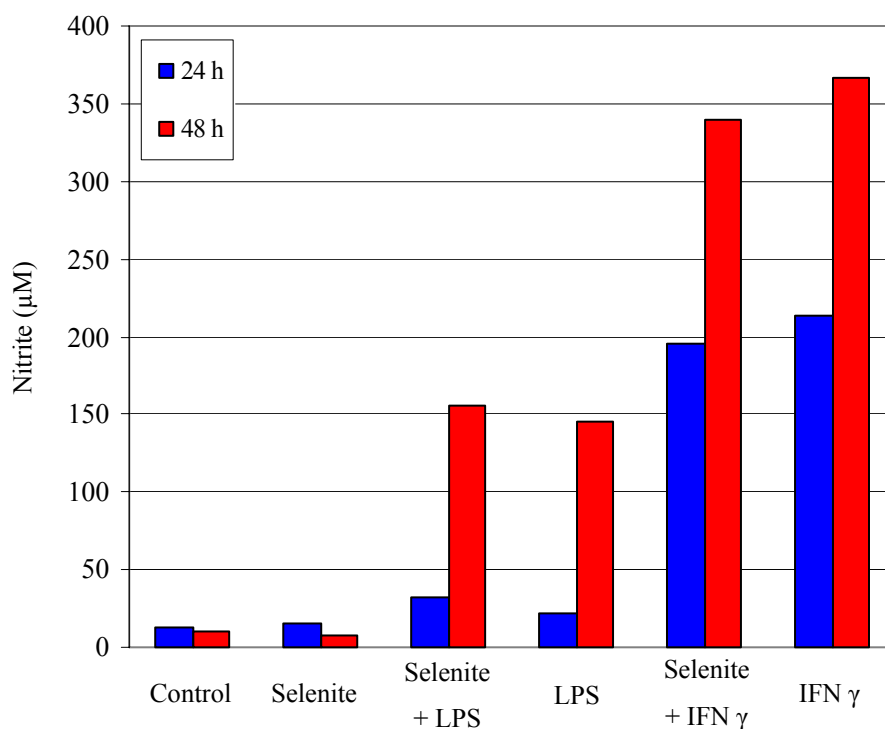


Figure 27 The effect of selenium on the release of NO induced by 10 $\mu\text{g/ml}$ LPS and 50 U/ml IFN γ was measured after 24 and 48 hours. Selenium was added as Na_2SeO_3 (500 nM) 24 hours before stimulation.

In conclusion, the pre-treatment with selenite did not influence the LPS- and IFN γ -induced NO production and cell death, in contrast to the effects observed after H_2O_2 treatment. This indicates different mechanisms of activation and induction of cell death triggered by the substances used.

5.13 Construction of plasmids for the regulation of Gpx1 expression

The previous results have shown that selenium, added as sodium selenite, protects microglial BV2 cells against activation and oxidative stress induced by hydrogen peroxide. These effects are related to the capability of selenium to be incorporated into selenoproteins as the amino acid selenocysteine. It has also been shown that the addition of selenite (in the protective range concentration) induced very quickly the expression of the classic glutathione peroxidase (Gpx1). In order to find out whether Gpx1 is the selenoprotein responsible for these effects, a molecular biological approach was engaged. For this purpose plasmids were produced which overexpress or downregulate the expression of Gpx1.

In the following section the cloning of the constructs will be described.

5.13.1 Cloning of the Gpx1-EGFP-C1 vector

In order to overexpress the glutathione peroxidase 1 protein, a construct containing an enhanced green fluorescent protein (EGFP) was generated using the pEGFP-C1 vector for eukaryotic expression. This construct was used to produce eukaryotic cells that overexpress Gpx1 (Gpx1-EGFP-C1) as a recombinant protein.

The flow chart outlining the cloning strategy is presented in Figure 28. The Gpx1 gene was amplified from a mouse DNA template by PCR and first cloned into the pCR[®] 2.1-TOPO plasmid and then into the pEGFP-C1 expression vector.

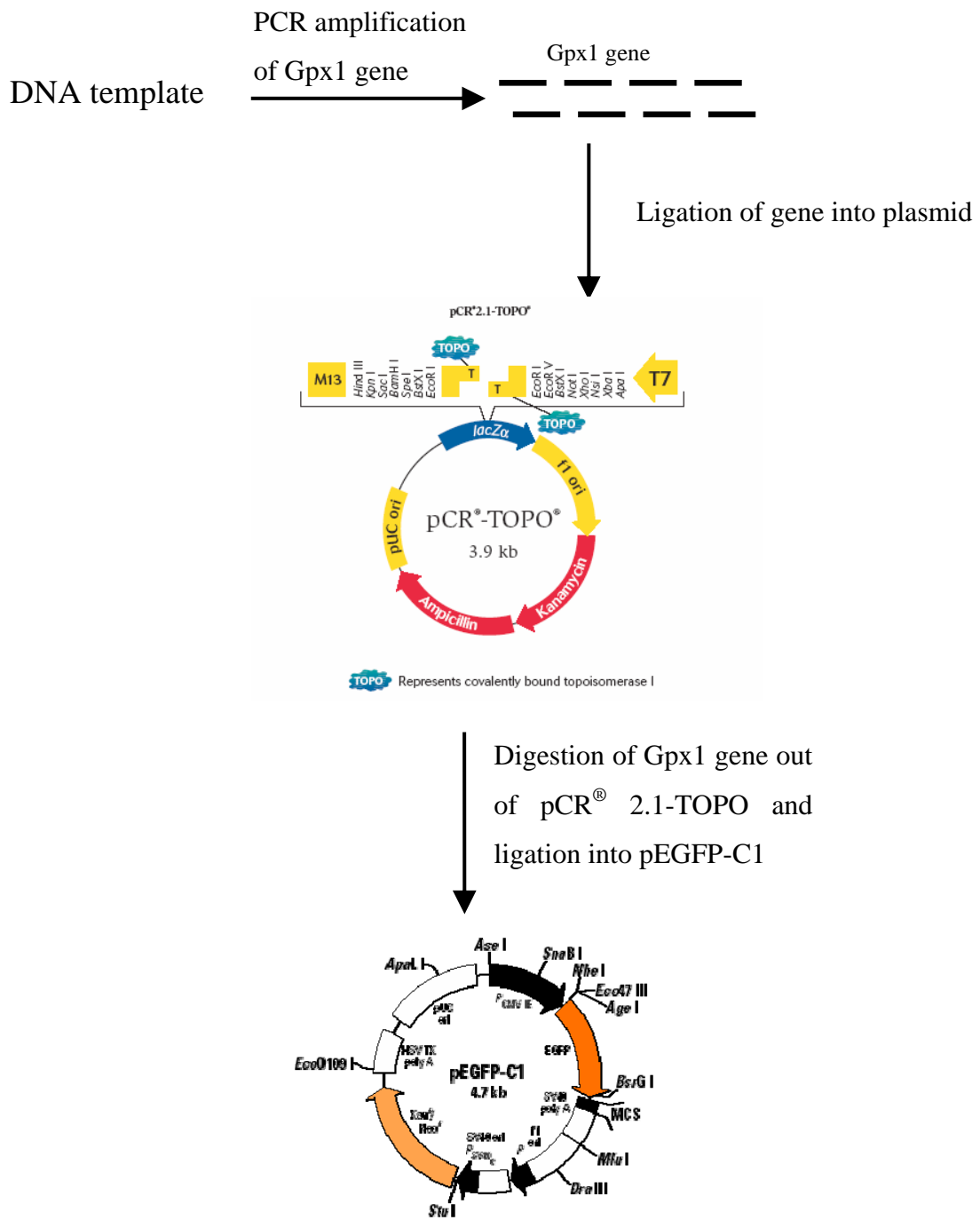


Figure 28 Flow chart of Gpx1-EGFP-C1 molecular cloning. Maps of pCR[®] 2.1-TOPO and pEGFP-C1 vectors (with restriction site) are shown.

Analysis of the Gpx1 sequence

The Gpx1 mRNA sequence was obtained from the NCBI. It is shown in Figure 29. The Gpx1 gene has 923 nucleotides, the CDS (protein-coding sequence), a coding sequence beginning at base 38 and ending at base 643, has a protein product of about 100 kDa. Coding start and stop codons are marked in red and blue boxes, respectively. The putative SECIS element is boxed in green.

```

1 agtacggatt ccacgtttga gtcccaacat ctccagtstartatg tgtgctgctc ggctctcegc
61 ggcgggcacag tccaccgtgt atgccttctc cgcgcgcccg ctgacgggcg gggagcctgt
121 gagcctgggc tccttgcggg gcaagggtgct gctcattgag aatgtcgcgt ctctdSECIStgagg
181 caccacgata cgggactaca ccgagatgaa cgatctgcag aagcgtctgg gacctcgtgg
241 actggtggtg ctccggtttcc cgtgcaatca gttcggacac caggagaatg gcaagaatga
301 agagattctg aattccctca agtacgtccg acctggtggc gggttcgagc ccaattttac
361 attgtttgag aagtgcgaag tgaatggtga gaaggctcac ccgctcttta ctttctgctg
421 gaatgccttg ccaacaccca gtgacgacc cactgcgctc atgaccgacc ccaagtacat
481 catttgggtc ccggtgtgcc gcaacgacat tgcttggaac tttgagaagt tcttgggtggg
541 ccccgacggt gttcccgtgc gcaggtacag ccgcccgttt cgtaccatcg acatcgaacc
601 tgacatagaa accctgctgt ccacgcagtc tggcaactccstoptaastopggcggcc ctggcattgg
661 cttggtgatt actSECISggctgca ctctgggggg cggttcttcc atgatggtgt ttcctctaaa
721 tttgcaSECIScggg gaaacacctg atttccagga aaatcccctc agatgggcgc tggteccatc
781 cattcccgat gcctttccac ctaatgaaag gtggtttcac tactaagaat aaagtgctga
841 atatcagaat tgtttgtgtg tctgtgtca ttgtcacctt ttggatagcc tcatagtcag
901 ggataaggaa ctcaatccca gag

```

Figure 29 The complete nucleotide sequence of the mus musculus glutathione peroxidase 1 (Gpx1) gene (mRNA). The cDNA is 923 bp long, the start codon is boxed in red, stop codon in blue. The TGA at 176 (boxed in black) does not work as a stop codon, but encodes for a SeCys, because of the presence of the SECIS element in the 3'UTR region (SECIS element is boxed in green). GenBank Accession number NM_008160.

Gpx1 PCR

The mouse HT22 cDNA containing the intact Gpx1 gene was used as PCR template. For that purpose two specific primers were designed to amplify the full-length cDNA by PCR. The amplified cDNAs include a large portion of the 3'-UTR region with the respective SECIS element in order to obtain the full size selenoprotein.

The forward primer design for the cloning of the full length sequence introduces an Hind III site and the reverse primer introduces a Bam HI restriction site. The sequence of the purchased oligonucleotides used is shown in Table 6.

<i>Primer</i>	<i>Sequence</i>	<i>Accession No./ Amplified fragment (bp)</i>
Gpx1-GFP-F	Hind III 5'- AAGCTT CGATGTGTGCTGCTCG-3'	NM_008160/784
Gpx1-GFP-R	Bam HI 5'-GGATCCGTAGTGAAACCACCTTTCA-3'	

Table 6 Primers used for PCR amplification of Gpx1 (restriction sites are indicated). Gpx1-GFP-F is the forward primer, Gpx1-GFP-R the reverse. These primers permit to amplify the Gpx1 full length cDNA, including the SECIS element and create Hind III and Bam HI restriction sites. The amplified region corresponds to 784 bp.

The desired PCR product was obtained with the following PCR-program (Table 7) on a thermocycler, using a Taq polymerase with cDNA from mouse HT22 cells as template and the specially designed primers. A negative control without template was also prepared. The PCR mixtures were denatured by heating at 94 °C, then cooled to allow the oligonucleotide primers to anneal to their target sequence. Finally the annealed primers were extended with DNA polymerase. The cycle of denaturation, annealing and DNA synthesis was repeated for 30 cycles, so that the products of one round of amplification served as templates for the next, doubling the amount of desired DNA product in each round.

DURATION	TEMPERATURE	CYCLES
3 minutes	94 °C	1
20 seconds	94 °C	2
40 seconds	53 °C	
1 minute	72 °C	
30 seconds	94 °C	30
40 seconds	61 °C	
1 minute	72 °C	
∞	4 °C	

Table 7 PCR program used for amplification of full length Gpx1.

PCR-amplified products were then run on a 1.5 % agarose gel. Figure 30 shows that the PCR was very specific (lane 1) and the major product formed corresponded to about 800 bp (the expected size was 784 bp). The control PCR (lane 3), without DNA, showed no product formed. In the gel, a λ DNA ladder was run next to the PCR product. A ladder is a mixture of fragments with known size to be compared with the PCR fragments.

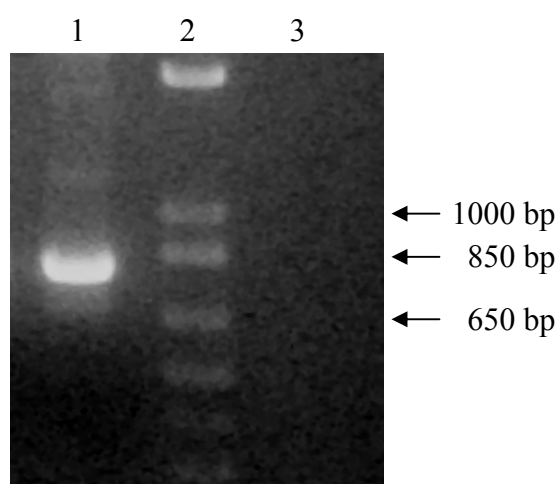


Figure 30 Verification of the PCR product on a gel. Lane 1: The PCR fragment is approximately 800 bases long. Lane 2: λ DNA ladder. Lane 3: Negative control.

TOPO TA cloning

The band corresponding to about 800 bp was excised and purified according to the standard protocol of NucleoSpin[®] Extract II.

The purified PCR product was cloned into a pCR2.1-TOPO vector: The TOPO TA cloning kit provides a highly efficient cloning strategy for the direct insertion of *Taq* polymerase-amplified PCR products into a plasmid vector. The TOPO cloning reaction was set up, and transformed into One shot Competent Cell as described in the Method section. Four white colonies were cultured overnight in 2x YT medium containing ampicillin, and the plasmid DNA was isolated using the mini-purification method which allows a quick purification step. The plasmids were subsequently analyzed by restriction analysis to confirm the presence of the insert. *Hind III* and *Bam HI* restriction enzymes were used. Figure 31 shows the resulting agarose gel after digestion: the upper bands represent the pCR2.1-TOPO vector (about 3.9 kb), the lower band is the Gpx1 insert (about 800 bp). All four clones were correct and had the right insert size. Therefore a glycerol stock of each clone for long-term storage was prepared and stored at -80°C .

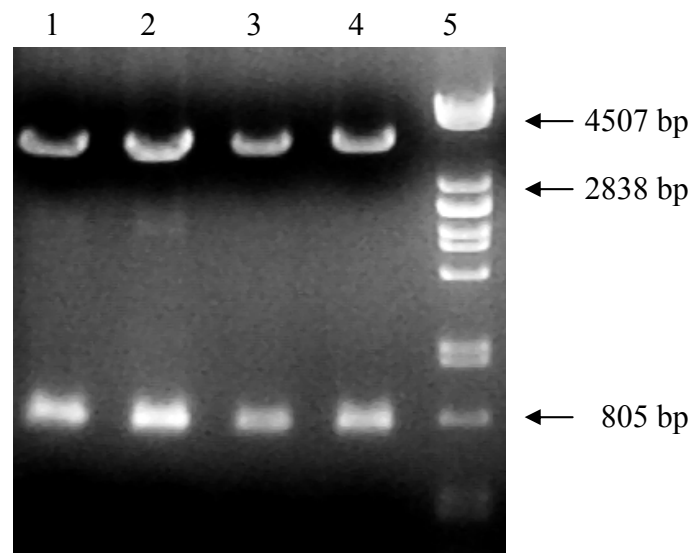


Figure 31 Agarose gel after restriction digestion of four isolated plasmids (lane 1 to 4). Vector: pCR2.1-TOPO (~3.9 kb). Lane 5: λ DNA ladder. All four selected clones contained an insert about 800 bp long.

The Gpx1 - pCR2.1-TOPO plasmid was used as an intermediate step between PCR amplification of the gene and ligation into the intended plasmid in order to make sure that the insert had the desired size, restriction enzyme recognition sites and orientation. The intended plasmid was the pEGFP-C1 vector, used to express GFP at the N-terminus of Gpx1. For this purpose, large amounts of the Gpx1 - pCR2.1-TOPO plasmid and the pEGFP-C1 vector were cut with the same restriction enzymes in order to produce insert and vector, respectively, with cohesive ends for the ligation.

Figure 32 shows the maxi-restriction digestion designed for obtaining large amounts of the insert and carried out as described in the method section. As expected, an intense band at 800 bp was formed which was visualized in the gel (Figure 32, lanes 1 to 4); the upper band represents the empty pCR2.1-TOPO plasmid.

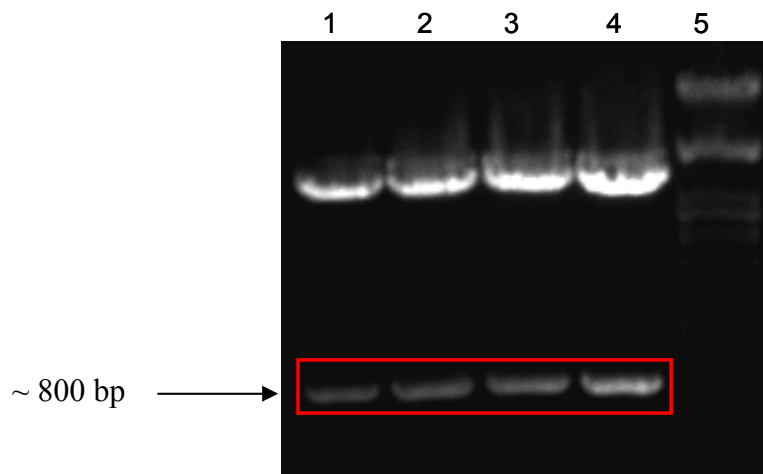


Figure 32 Agarose gel of maxi-digestion of Gpx1 - pCR2.1-TOPO (lane 1 to 4). The bands boxed in red are the Gpx1 insert DNA out of the pCR2.1-TOPO vector. Lane 5: λ DNA ladder.

Figure 33 shows the agarose gel of the pEGFP-C1 maxi digestion. A strong band was observed at about 4700 bp representing the cut linearized vector, indispensable for cloning the Gpx1 insert.

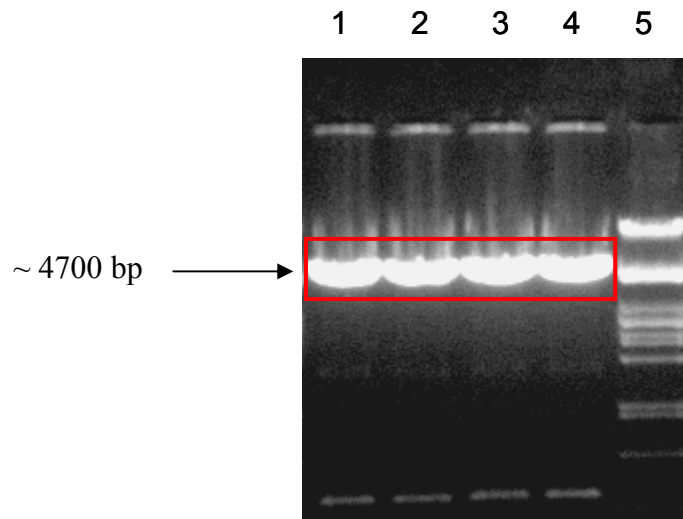


Figure 33 Agarose gel of maxi-digestion pEGFP-C1 (lane 1 to 4). The bands boxed in red are the linearized vector digest with *Hind III* and *Bam HI*. Lane 5: λ DNA ladder.

Insert and vector DNA were purified from the respective agarose gels. The DNA sample concentrations were estimated by running a small known volume of the cut purified insert and vector DNA on an agarose gel adjacent to a DNA marker with known DNA band amounts (shown in Figure 34). The Gpx1 insert DNA concentration was estimated as 32 ng/ μ l, the EGFP-C1 vector as about 300 ng/ μ l.

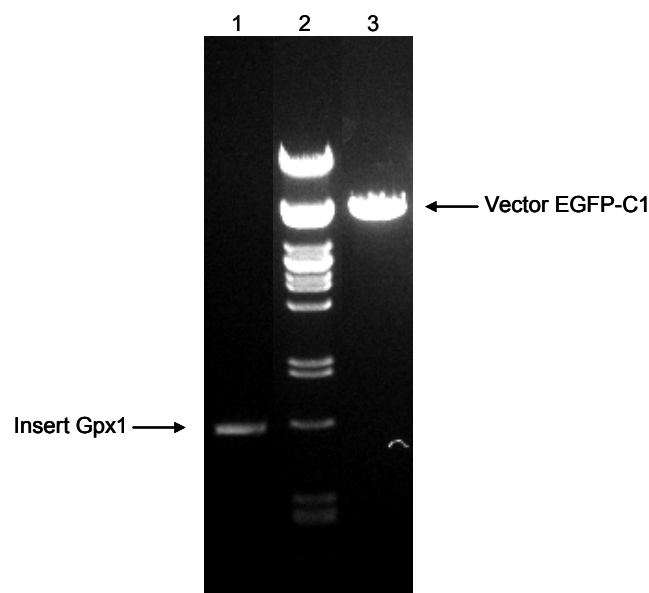


Figure 34 Determination of the DNA concentration by agarose gel electrophoresis. Insert Gpx1 (lane 1) and vector EGFP-C1 (lane 3) DNA were run next to a λ DNA ladder (lane 2) to compare the intensity of the ethidium bromide bands.

The vector EGFP-C1 was dephosphorylated and the ligation was performed using 200 ng of the vector and 115 ng of the Gpx1 insert. The ligation reaction was transformed in competent *E. Coli*. 8 colonies were examined for positive plasmids. A restriction enzyme digestion was employed to verify the cloning strategy. Once the restriction digest was completed, agarose gel electrophoresis was performed to separate and visualize the digest fragments by size (Figure 35). The correct patterns after the restriction enzyme digestion indicated a successful cloning. Each selected plasmid contained the right insert about 800 bp long.

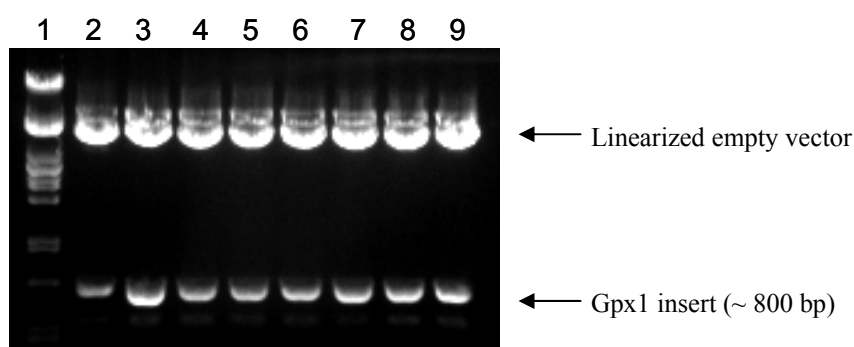


Figure 35 Agarose gel electrophoresis of Gpx1-EGFP-C1 DNA mini-purification digested with Hind III and Bam HI. Lane 1: λ DNA ladder. Lane 2 to 9: selected clones.

The plasmid Gpx1-EGFP-C1 number 3 (lane 4 on the agarose gel) was chosen and purified using the NucleoBond Plasmid Maxi EF kit. The concentration of Gpx1-EGFP-C1 DNA was determined by spectrophotometric estimation. It was diluted to a final concentration of 1 $\mu\text{g}/\mu\text{l}$. The A_{260}/A_{280} ratio was calculated as 1.90, which indicated a good level of purity of the DNA, without contamination by protein or organic chemicals.

An aliquot of the Gpx1-EGFP-C1 purified plasmid was sequenced by MWG Biotech AG to verify that it contains the desired insert. Figure 36 and Figure 37 show the results of the BLAST search, the alignment was found to be excellent (99 %). The Gpx1-EGFP-C1 plasmid was used for the following transfection experiments to over-express a recombinant protein, which expressed GFP at the N-terminus of Gpx1.

```

Sequence Mus musculus glutathione peroxidase 1 (Gpx1), mRNA. Length = 923

Score = 1506 bits (783), Expect = 0.0
Identities = 785/786 (99%)
Strand = Plus / Minus

Query: 38  atgtgtgctgctcggctctccgcggcggcacagtccaccgtgatgccttctccgcgcgc 97
          |||
Sbjct: 832 atgtgtgctgctcggctctccgcggcggcacagtccaccgtgatgccttctccgcgcgc 773

Query: 98  ccgctgacggcgaggagcctgtgagcctgggctcctgcggggcaaggctgctcatt 157
          |||
Sbjct: 772 ccgctgacggcgaggagcctgtgagcctgggctcctgcggggcaaggctgctcatt 713

Query: 158 gagaatgtcgcgtctctctgaggcaccacgatccgggactacaccgagatgaacgatctg 217
          |||
Sbjct: 712 gagaatgtcgcgtctctctgaggcaccacgatccgggactacaccgagatgaacgatctg 653

Query: 218 cagaagcgtctgggacctcgtggactgggtgctcggtttcccgtgcaatcagttcggga 277
          |||
Sbjct: 652 cagaagcgtctgggacctcgtggactgggtgctcggtttcccgtgcaatcagttcggga 593

Query: 278 caccaggagaatggcaagaatgaagagattctgaattccctcaagtacgtccgacctggt 337
          |||
Sbjct: 592 caccaggagaatggcaagaatgaagagattctgaattccctcaagtacgtccgacctggt 533

Query: 338 ggcgggttcgagcccaattttacattgtttgagaagtgcgaagtgaatggtgagaaggct 397
          |||
Sbjct: 532 ggcgggttcgagcccaattttacattgtttgagaagtgcgaagtgaatggtgagaaggct 473

Query: 398 caccgcgtctttaccttccctgcggaatgccttgccaacaccagtgacgacccactgcg 457
          |||
Sbjct: 472 caccgcgtctttaccttccctgcggaatgccttgccaacaccagtgacgacccactgcg 413

Query: 458 ctcatgaccgaccccaagtacatcatttggctcctcgggtggtgccgcaacgacattgcctgg 517
          |||
Sbjct: 412 ctcatgaccgaccccaagtacatcatttggctcctcgggtggtgccgcaacgacattgcctgg 353

Query: 518 aactttgagaagttcctggtgggccccgacggtgttcccgtgcgcaggtaacagccgccgc 577
          |||
Sbjct: 352 aactttgagaagttcctggtgggccccgacggtgttcccgtgcgcaggtaacagccgccgc 293

Query: 578 tttcgtaccatcgacatcgaacctgacatagaaacctgctgtcccagcagtctggcaac 637
          |||
Sbjct: 292 tttcgtaccatcgacatcgaacctgacatagaaacctgctgtcccagcagtctggcaac 233

Query: 638 tcctaagcggccctggcattggcttggtgattactggctgactctggggggcggttct 697
          |||
Sbjct: 232 tcctaagcggccctggcattggcttggtgattactggctgactctggggggcggttct 173

Query: 698 tccatgatggtgtttcctctaaatttgacggagaaacacctgatttccaggaaaatccc 757
          |||
Sbjct: 172 tccatgatggtgtttcctctaaatttgacggagaaacacctgatttccaggaaaatccc 113

Query: 758 ctccagatggcgctggtcccatccattcccgatgcctttccacctaataaagggtggttt 817
          |||
Sbjct: 112 ctccagatggcgctggtcccatccattcccgatgcctttccacctaataaagggtggttt 53

Query: 818 cactac 823
          |||
Sbjct: 52 tactac 47

```

Figure 36 Sequences alignment using Blast engine for local alignment. Gpx1-EGFP-C1 DNA from Maxi prep was sequenced by MWG Biotech Company using EGFP-C1-Gpx1-pEGFP-C1rev primer: the resulting sequence (Sbjct) was compared with the known sequence of Gpx1 (Query). The identity was 99 %.

```

Sequence Mus musculus glutathione peroxidase 1 (Gpx1), mRNA. Length = 923

Score = 1506 bits (783), Expect = 0.0
Identities = 785/786 (99%)
Strand = Plus / Plus

Query: 38  atgtgtgctgctcggctctccgcgccggcacagtcaccctgtatgccttctccgcgcgc 97
          |||
Sbjct: 18  atgtgtgctgctcggctctccgcgccggcacagtcaccctgtatgccttctccgcgcgc 77

Query: 98  ccgctgacgggggggagcctgtgagcctgggctccctgcggggcaaggtgctgctcatt 157
          |||
Sbjct: 78  ccgctgacgggggggagcctgtgagcctgggctccctgcggggcaaggtgctgctcatt 137

Query: 158  gagaatgtcgcgtctctctgaggcaccacgatccgggactacaccgagatgaacgatctg 217
          |||
Sbjct: 138  gagaatgtcgcgtctctctgaggcaccacgatccgggactacaccgagatgaacgatctg 197

Query: 218  cagaagcgtctgggacctcgtggactggtggtgctcggtttcccgtagaatcagttcgga 277
          |||
Sbjct: 198  cagaagcgtctgggacctcgtggactggtggtgctcggtttcccgtagaatcagttcgga 257

Query: 278  caccaggagaatggcaagaatgaagagattctgaattccctcaagtagctccgacctggt 337
          |||
Sbjct: 258  caccaggagaatggcaagaatgaagagattctgaattccctcaagtagctccgacctggt 317

Query: 338  ggcgggttcgagcccaattttacattgtttgagaagtgcgaagtgaatggtgagaaggct 397
          |||
Sbjct: 318  ggcgggttcgagcccaattttacattgtttgagaagtgcgaagtgaatggtgagaaggct 377

Query: 398  caccgctctttaccttctcgtcggaatgccttgccaacacccagtgacgaccccaactgcg 457
          |||
Sbjct: 378  caccgctctttaccttctcgtcggaatgccttgccaacacccagtgacgaccccaactgcg 437

Query: 458  ctcatgaccgaccccaagtacatcatttggctcctcgggtgtgcccgaacgacattgcctgg 517
          |||
Sbjct: 438  ctcatgaccgaccccaagtacatcatttggctcctcgggtgtgcccgaacgacattgcctgg 497

Query: 518  aactttgagaagttcctggtgggccccgacggtgttcccgtagcaggtacagccgcccgc 577
          |||
Sbjct: 498  aactttgagaagttcctggtgggccccgacggtgttcccgtagcaggtacagccgcccgc 557

Query: 578  ttcgtaccatcgacatcgaaacctgacatagaaacctgctgtcccagcagctctggcaac 637
          |||
Sbjct: 558  ttcgtaccatcgacatcgaaacctgacatagaaacctgctgtcccagcagctctggcaac 617

Query: 638  tcctaaggcggccctggcattggcttggctgattactggctgactctggggggcggttct 697
          |||
Sbjct: 618  tcctaaggcggccctggcattggcttggctgattactggctgactctggggggcggttct 677

Query: 698  tccatgatggtgttctcctaatttgacgggagaaacacctgatttccaggaaaatccc 757
          |||
Sbjct: 678  tccatgatggtgttctcctaatttgacgggagaaacacctgatttccaggaaaatccc 737

Query: 758  ctcatgagggcgctgggtccatccattcccgatgcctttcacctaataaagggtggttt 817
          |||
Sbjct: 738  ctcatgagggcgctgggtccatccattcccgatgcctttcacctaataaagggtggttt 797

Query: 818  cactac 823
          |||
Sbjct: 798  tactac 803

```

Figure 37 Sequences alignment using Blast engine for local alignment. Gpx1-EGFP-C1 DNA from Maxi prep was sequenced by MWG Biotech Company using EGFP-C1-Gpx1-pEGFP-C1 for primer: the resulting sequence (Sbjct) was compared with the known sequence of Gpx1 (Query). The identity was 99 %.

5.13.2 Cloning of siRNA vectors

The introduction of double-stranded small interfering RNA (siRNA) into a cell is an efficient method to repress post-transcriptionally the expression of a gene. The pSUPER RNAi system (Oligoengine, Seattle, WA; www.oligoengine.com) was used to ablate specifically the glutathione peroxidase 1 protein. The system provides a mammalian expression vector that directs intracellular synthesis of siRNA transcripts causing efficient and specific gene silencing (107). For this purpose, three different siRNA plasmids were constructed.

Potential siRNA target sequences in the mouse Gpx1 mRNA were identified as described in the Method section:

bases	sequence
142-161:	AGGTGCTGCTCATTGAGAA
292-311:	AGAATGAAGAGATTCTGAA
293-312:	GAATGAAGAGATTCTGAAT

Each target sequence was tested in silico to avoid silencing of multiple genes (off-target effects). The analysis of these sequences using the software BLAST (NCBI) showed that they were specific for the Gpx1 protein.

According to the pSUPER RNAi system, two 64-nt oligonucleotides (forward and reverse) were synthesized for each target region.

1. mGPX1 RNAi¹⁴²

Target sequence sense: AGGTGCTGCTCATTGAGAA

Target sequence antisense: TTCTCAATGAGCAGCACCT

Forward primer mGPX1 RNAi¹⁴²:

5' GATCCCCAGGTGCTGCTCATTGAGAAttcaagagaTTCTCAATGAGCAGCACCTt
ttttggaaa-3'

Reverse primer mGPX1 RNAi¹⁴²:

5´ agcttttccaaaaa AGGTGCTGCTCATTGAGAA TCTCTTGAA TTCTCAATGAGCA
GCACCTggg-3´

2. mGPX1 RNAi²⁹²

Target sequence sense: AGAATGAAGAGATTCTGAA

Target sequence antisense: TTCAGAATCTCTTCATTCT

Forward primer mGPX1 RNAi²⁹²:

5´ GATCCCC AGAATGAAGAGATTCTGAA ttcaagaga TTCAGAATCTCTTCATTCT t
ttttggaaa-3´

Reverse primer mGPX1 RNAi²⁹²:

5´ agcttttccaaaaa AGAATGAAGAGATTCTGAA TCTCTTGAA TTCAGAATCTCTT
CATTCTggg-3´

3. mGPX1 RNAi²⁹³

Target sequence sense: GAATGAAGAGATTCTGAAT

Target sequence antisense: ATTCAGAATCTCTTCATTCT

Forward primer mGPX1 RNAi²⁹³:

5´ GATCCCC GAATGAAGAGATTCTGAAT ttcaagaga ATTCAGAATCTCTTCATTCT t
ttttggaaa-3´

Reverse primer mGPX1 RNAi²⁹³:

5´ agcttttccaaaaa GAATGAAGAGATTCTGAAT TCTCTTGAA ATTCAGAATCTCT
TCATTCTggg-3´

Single-stranded forward and reverse siRNA pairs were annealed to get complementary siRNA duplex. Annealed oligonucleotides were then ligated into the pSUPER-GFP vector.

The pSuper-GFP vector contained ampicillin resistance genes to enable the antibiotic selection. The vector uses the polymerase-III H1-RNA gene promoter that produces small RNA transcripts lacking a polyA tail.

Recombinant plasmid constructs were then transformed into *E. Coli* and screened for positive clones. 8 colonies for each construct were picked and mini-prep was carried out in order to locate a positive clone (i.e. containing vector with oligo insert). The purified DNA was then subjected to restriction digestion with *EcoRI* and *HindIII*. After digestion, a positive clone had a fragment of approximately 290 bp in length. The analysis of the fragments on an agarose gel (Figure 38) revealed that only one clone was positive for Gpx1-pSUPER-142, three for Gpx1-pSUPER-293 and no positive clone was found for Gpx1-pSUPER-292.

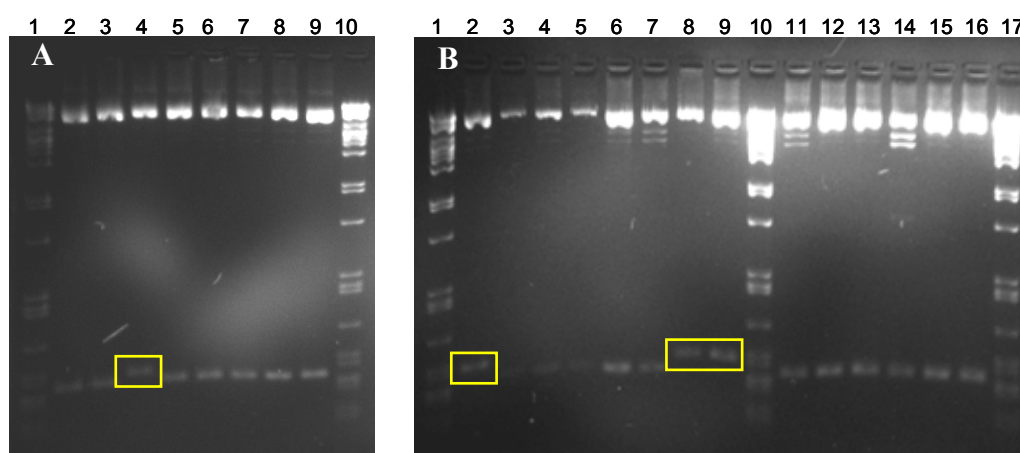


Figure 38 Agarose gel (2 %) of mini-prep of siRNA plasmids after restriction digestion with *EcoRI* and *HindIII*. A) Lanes 1 and 10: λ DNA ladder. Lanes 2 to 9: analysis of Gpx1-pSUPER-142 clones. B) Lanes 1, 10 and 17: λ DNA ladder. Lanes 2 to 9: Gpx1-pSUPER-293 and lanes 11 to 16: Gpx1-pSUPER-292 clones. The positive clones revealed a band of approximately 290 bp in length (boxed in yellow).

Plasmid purification of the positive clones (Gpx1-pSUPER-142: lane 4 of Figure 38-A; Gpx1-pSUPER-292: lane 2 Figure 38-B) was performed using the NucleoBond Plasmid Maxi EF kit. The DNA of each Maxi-prep was digested again with *EcoRI*

and *HindIII* restriction enzymes and analysed on an agarose gel to prove the integrity of the DNA.

Finally, the presence of the correct insert within the recombinant pSUPER-GFP vector was confirmed by DNA sequencing and BLAST search (Figure 39 and Figure 40).

The DNA concentration was determined spectrophotometrically. It was diluted to a final concentration of 1 µg/µl. Each plasmid showed a good grade of purity: the A_{260}/A_{280} ratio was about 1.85.

```

query: Forward mGPX1 RNAi142
Score = 123 bits (64), Expect = 3e-26
Identities = 64/64 (100%)
Strand = Plus / Minus

Query: 1   gatccccaggtgctgctcattgagaattcaagagattctcaatgagcagcaccttttttg 60
          |||
Sbjct: 118 gatccccaggtgctgctcattgagaattcaagagattctcaatgagcagcaccttttttg 59

Query: 61   gaaa 64
          |||
Sbjct: 58   gaaa 55

```

Figure 39 Sequences alignment using Blast engine for local alignment. Forward mGpx1 RNAi¹⁴² DNA was sequenced by MWG Biotech Company using M13_rev primer: the resulting sequence (Sbjct) was compared with the original 64-nt oligo designed sequence. The identity was 100 %.

```

query: Forward mGPX1 RNAi293
Score = 123 bits (64), Expect = 3e-26
Identities = 64/64 (100%)
Strand = Plus / Minus

Query: 1   gatccccgaatgaagagattctgaatttcaagagaattcagaatctcttcattctttttg 60
          |||
Sbjct: 127 gatccccgaatgaagagattctgaatttcaagagaattcagaatctcttcattctttttg 68

Query: 61   gaaa 64
          |||
Sbjct: 67   gaaa 64

```

Figure 40 Sequences alignment using Blast engine for local alignment. Forward mGpx1 RNAi²⁹³ DNA was sequenced by MWG Biotech Company using M13_rev primer: the resulting sequence (Sbjct) was compared with the original 64-nt oligo designed sequence. The identity was 100 %.

5.14 Transfection experiments

5.14.1 Establishment of transient transfection of COS-7 cells with Gpx1-EGFP-C1 DNA

Before applying this strategy to the BV2 cells, an optimization of the translation efficiency of the Gpx1-EGFP-C1 plasmid in COS-7 cells was necessary.

COS-7 cells are a popular research tool, especially for transfection experiments with recombinant plasmids. The COS-7 cell line is an adherent kidney cell line derived from African green monkey kidney.

The GFP reporter gene was used to quantify the efficacy of transfection and to monitor the amount of protein being synthesized from the introduced vector. Such an analysis is shown in Figure 41, where COS-7 cells were transfected with different amounts of DNA. The images were taken on a fluorescent microscope, which provides the easiest method for the detection of EGFP expression and enables the analysis of living cells. This result showed that the introduced vector, which expresses Gpx1 as a fusion protein with green fluorescent protein, had no influence on the viability of the cells. Furthermore the morphology of COS-7 cells was the same after transfection of the pEGFP-C1 empty vector or the Gpx1-EGFP-C1 plasmid. The optimum quantity of DNA necessary to induce a successful transfection was found to be 5 μg for the pEGFP-C1 empty vector and 30 μg for the Gpx1-EGFP-C1.

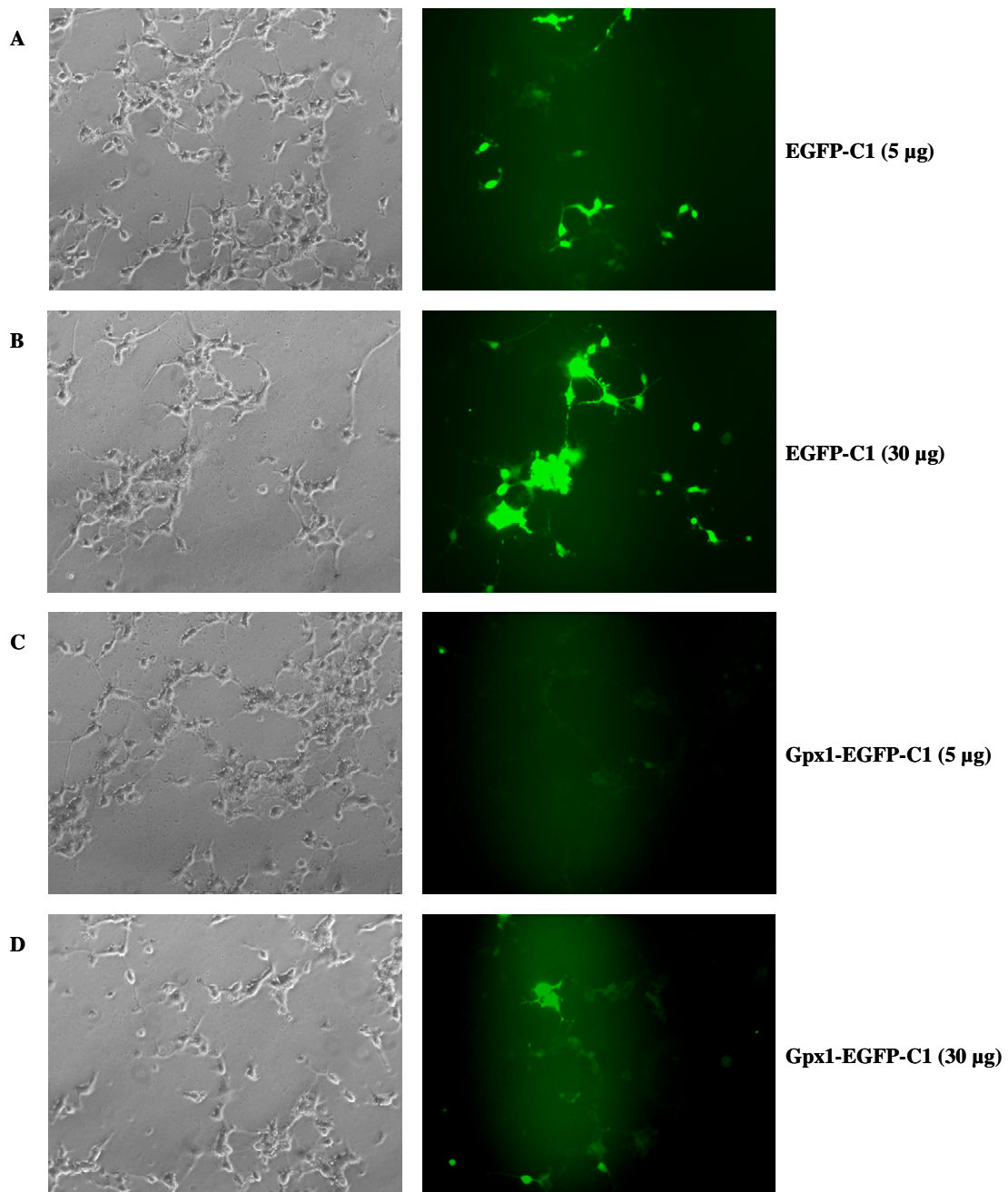


Figure 41 DNA transfer with the calcium phosphate method in COS-7. A collage of images of GFP fluorescence of COS-7 cells, taken 48 hours after transfection, shows efficacy of 5 µg EGFP-C1 DNA and 30 µg Gpx1-EGFP-C1 DNA. A and B: cells transfected with 5 and 30 µg EGFP-C1 DNA, respectively. C and D: cells transfected with 5 and 30 µg Gpx1-EGFP-C1 DNA, respectively. Left: phase microscopy. Right: cells imaged under GFP fluorescence.

COS-7 cells transfected with different quantities of DNA were harvested 48 hours after transfection and the total protein was extracted. Equal amounts of protein lysate (20 μg) were subjected to SDS-PAGE and transferred to a blot membrane, which was subsequently incubated with the anti- *Aequorea Victoria* GFP antibody. Figure 42 shows the scanned ECL film after development. On the left side are samples of cells transfected with the EGFP-C1 empty vector, which induces the expression of GFP protein (Mw ~ 27 kDa). On the right side are proteins from cells transfected with the Gpx1-EGFP-C1 vector which induces the expression of GFP-tagged Gpx1. The transient expression of the fusion protein was predicted to result in a 52 kDa selenoprotein.

Together, these data showed that 5 μg of the EGFP-C1 empty vector DNA and 30 μg of the Gpx1-EGFP-C1 DNA are the optimum quantity to obtain a good transfection and a good expression level of proteins.

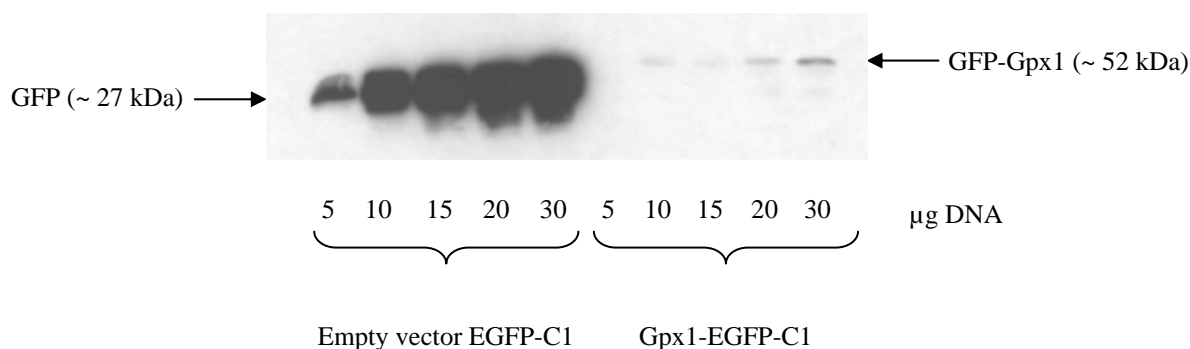


Figure 42 Western blot of COS-7 cell lysate after transient calcium phosphate transfection. Cells were transfected with the EGFP-C1 empty vector (5 to 30 μg DNA) and with the Gpx1-EGFP-C1 plasmid (5 to 30 μg DNA). Homogenates were subjected to SDS-PAGE and transferred onto a nitrocellulose membrane. Primary antibody: mouse anti *Aequorea Victoria* GFP (dilution 1:2500); secondary antibody: ECL anti-mouse IgG, peroxidase linked (1:5000).

5.14.2 Transfection of siRNA plasmids.

Gpx1-pSUPER-142 siRNA reduces Gpx1 expression

The ability of small interfering RNAs (siRNAs) to silence gene expression is proving to be invaluable for studying the gene function in cultured mammalian cells. siRNAs

can be transiently transfected into mammalian cells using commonly available transfection reagents.

Constructs of the two 19 nt sequences selected for targeting the knockdown of mouse Gpx1 (pSUPER-Gpx1-142 and pSUPER-Gpx1-293) were examined for their ability to reduce the Gpx1 protein level in COS-7 cells. The plasmids were co-transfected with Gpx1-EGFP-C1 in COS-7 cells using the calcium phosphate method. As control, the Gpx1-EGFP-C1 plasmid was also included in this experiment. The good transfection rate is shown in Figure 43.

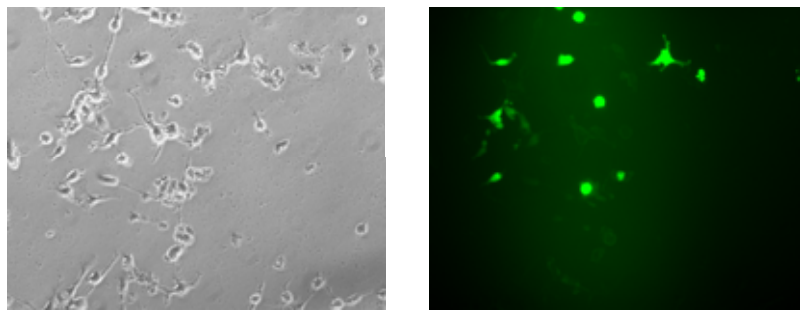


Figure 43 COS-7 cell images after transfection with Gpx1-EGFP-C1 plasmid. Left: phase microscopy. Right: cells imaged by GFP fluorescence. This result showed a successful transfection rate.

Proteins were harvested from the cells 24 hours post transfection and analyzed by Western blotting using anti-GFP antibody and anti- β -actin as load control.

Figure 44 shows the resulting Western blot against Aequorea Victoria GFP, which detects fusion constructs (GFP tagged proteins) and can be used to identify and confirm fusion proteins in mammalian cells.

It was noted that the pSUPER-Gpx1-142 siRNA construct (lane 2) reduced the expression of the targeted Gpx1 protein. The band corresponding to GFP-Gpx1 (52 kDa) was negligible as compared with the control (indication of a good silencing effect). The GFP protein (band at 27 kDa) was well expressed in both siRNA transfected cells, pSUPER-Gpx1-142 and pSUPER-Gpx1-293: that means the plasmids were effectively transfected because the pSUPER vector induces the expression of the GFP protein. pSUPER-Gpx1-293 did not seem to down-regulate the Gpx1 expression.

pSUPER-Gpx1-142 and pSUPER-Gpx1-293 (siRNA plasmids) showed different silencing efficiencies, which can be explained by either the nucleotide composition of the siRNA duplex by itself or by the targeted position within the mRNA. The positional effect can be attributed to the inaccessibility of the target site due to the secondary structure of mRNA or to the binding of regulatory proteins.

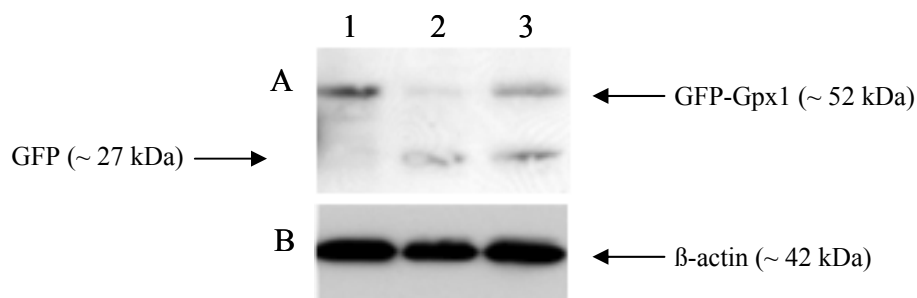


Figure 44 Western blot of COS-7 cell homogenates after transfection with the 30 μ g DNA (calcium phosphate method). Lysates were analyzed using anti Aequorea Victoria GFP antibody (A) at 1:2500 dilution and anti β -actin (B) at 1:500 dilution. Each lane contained 20 μ g proteins. The cells were transfected with: Lane 1: Gpx1-EGFP-C1 plasmid, 30 μ g. Lane 2: Gpx1-EGFP-C1 15 μ g + pSUPER-Gpx1-142 15 μ g. Lane 3: Gpx1-EGFP-C1 15 μ g + pSUPER-Gpx1-293 15 μ g. B) The membrane was stripped and reloaded with anti β -actin antibody as load control.

The possibility of having some unspecific silencing effects cannot be excluded even when the siRNAs are carefully selected. The following experiment was carried out in order to determine if the siRNA plasmids were specific for the Gpx1 protein down-regulation or if they influenced the expression of other selenoproteins. A simple means of monitoring selenoprotein synthesis is labelling of the transfected cells with ^{75}Se and separation of the labelled proteins by gel electrophoresis. BV2 cells were transfected using the electroporation method with pSUPER-Gpx1-142, pSUPER-Gpx1-293 and empty vector pSUPER-GFP as controls. One day after transfection, ^{75}Se -selenite (2 kBq/ml) was added to each plate (about 0.027 nM Se). 48 hours later total protein extracts were prepared. About 100 μ g protein were run on SDS-PAGE and the resulting gel was dried and exposed to a photostimulable phosphor plate for 5 days. Figure 45 shows the autoradiogram obtained in which several selenoprotein bands could be distinguished. The selenoprotein pattern was described previously. A quantitative analysis of the selenoprotein expression level was performed using the

AIDA software which allows the calculation of the percentage of each single band (Figure 46).

Based on the intensity of the bands, the level of the 25 kDa protein (Gpx1) in pSUPER-Gpx1-142-transfected cells was 2-fold lower than in the pSUPER-GFP-transfected control cells. The expression of the other selenoproteins was not affected, indicating a good specificity of pSUPER-Gpx1-142.

The pSUPER-Gpx1-293 DNA reduced slightly the intensity of the 25 kDa band. No interferences with other selenoproteins were observed.

These results confirmed that the siRNA construct pSUPER-Gpx1-142 was functional and specific for glutathione peroxidase 1. Therefore, it was used for experiments on Gpx1 underexpression in BV2 microglial cells.

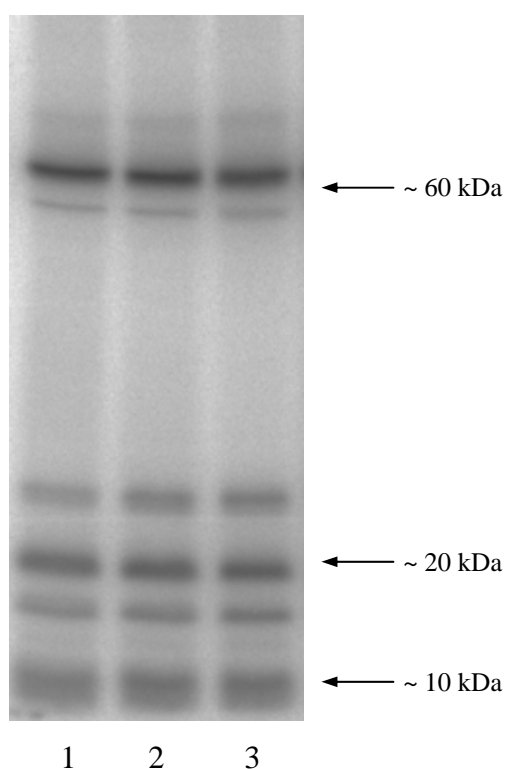


Figure 45 BV2 cells transfected with pSUPER-Gpx1-142 (lane 1), pSUPER-Gpx1-293 (lane 2) and pSUPER-GFP empty vector (lane 3) were treated with ^{75}Se -selenite for 48 hours before harvest. Selenoprotein levels in the cell lysates were analysed by separation on SDS-PAGE and autoradiography. The resulting audiogram is shown.

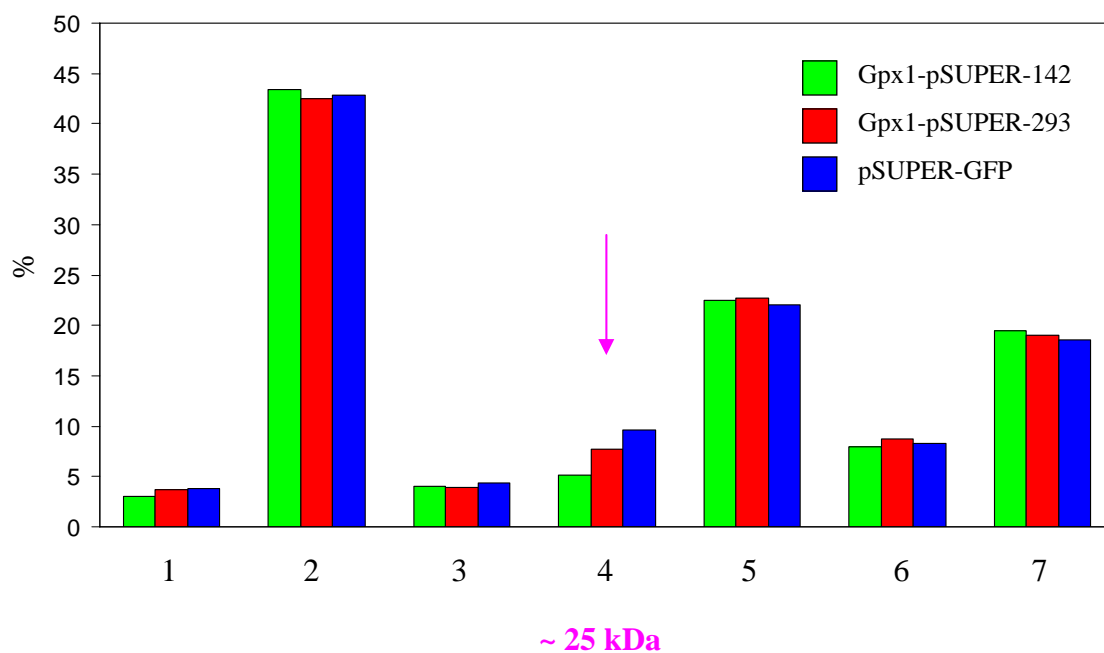


Figure 46 Quantification of the selenoprotein levels in BV2 cells after transfection with siRNA constructs (see caption Figure 45) Band intensities of the autoradiogram were calculated by densitometry using AIDA software and expressed as % of total selenoprotein activity.

In the same experiment, the morphology of BV2 cells 24 hours after-transfection was examined by phase contrast microscopy. As shown in Figure 47, the transfection with pSUPER-Gpx1-142 (siRNA) induced changes in the morphology of the cells. The cells lost their ramified form and were transformed into an amoeboid form.

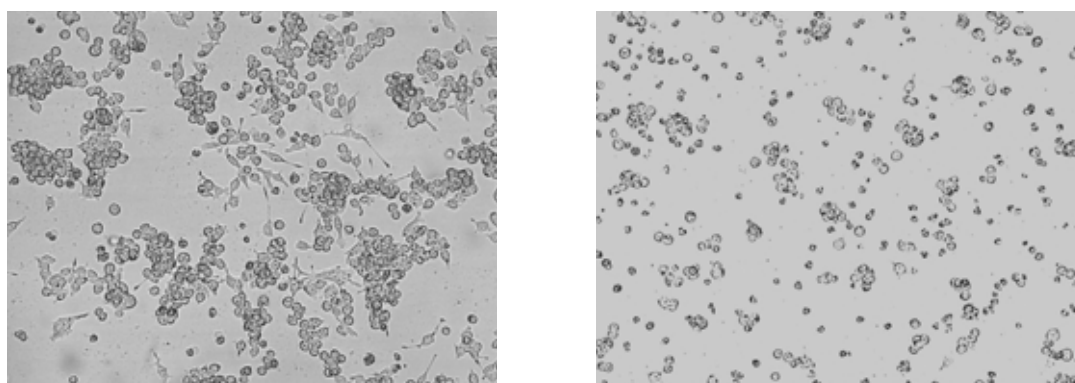


Figure 47 Morphological changes of BV2 cells transfected with the pSUPER-GFP vector (left) and with the empty pSUPER-Gpx1-142 (right). Phase contrast photographs of living BV2 cells 24 hours after transfection.

5.15 Effects of different Gpx1 levels on the microglial cells

Gpx1 was overexpressed and underexpressed in BV2 cell to determine whether the enzyme renders microglial cells less susceptible to cell death by peroxide treatment. The cells were transiently transfected with the respective plasmids which had been produced before (see section 5.13). The protection modulated by the expression of the Gpx1 protein was determined in BV2 microglial cells. The analysis of the protective role of Gpx1 during oxidative stress was performed by using the MTT cell viability test on the cells over- or under-expressing Gpx1.

5.15.1 Over-expression of Gpx1

The expression of Gpx1 was determined to investigate its involvement in the protective effect of sodium selenite supplementation in oxidative stress. Gpx1 was expressed as the GFP fusion protein by transfection of the Gpx1-EGFP-C1 construct. Cells were also transfected with the pEGFP-C1 empty vector as control. 24 hours after transfection, the cells were pre-treated with sodium selenite and then exposed to hydrogen peroxide as in the previous experiments. The cell viability results are shown in Figure 48. After exposure to H₂O₂, both Gpx1-overexpressed cells (A) and control cells (B) showed a reduction in cell viability. In the Gpx1-overexpressed cells exposed to oxidative stress, the cell viability measured by the MTT test was not increased by pre-treatment with 500 nM selenite.

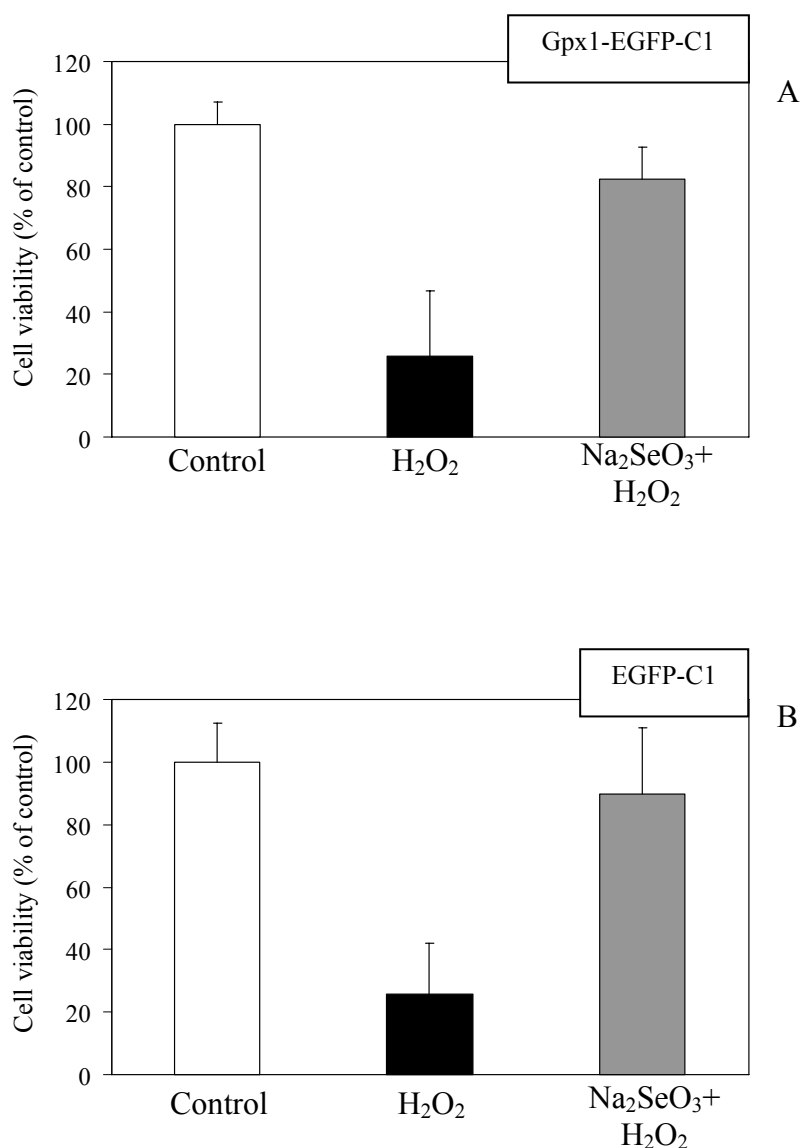


Figure 48 Effect of Gpx1 over-expression on BV2 cells exposed to oxidative stress. Cells were transfected with the Gpx1-EGFP-C1 plasmid (A) and the EGFP-C1 empty vector as control (B) using the electroporation technique. 24 hours after transfection, sodium selenite (500 nM for 24 hours) and/or H₂O₂ (250 μ M) were added and the MTT assay was performed as described previously.

These data show that over-expression of Gpx1 in BV2 cells had no particular effect on the protection against H₂O₂ damage. However the BV2 cells express in the normal state high levels of Gpx1 and may therefore be less responsive to an increase in the level of this protein.

5.15.2 Under-expression of Gpx1

This experiment was carried out to investigate the protective role of Gpx1 in microglial cells under oxidative stress conditions. The siRNA technology was used to suppress the Gpx1 expression of BV2 cells by transfection of the cloned vectors (see 5.13.2) into the cells. The susceptibility of Gpx1-under-expressing cells to H₂O₂, and their reactivity to selenite pre-treatment, was compared with the control cells, which are able to express all selenoproteins.

In cells under-expressing Gpx1 and in control cells, the cell viability after H₂O₂ treatment was assayed by the MTT test. Figure 49 shows three diagrams of the cell viability test in BV2 transfected with pSUPER-Gpx1-142 (A), pSUPER-Gpx1-293 (B) and with the empty vector pSUPER-GFP.

As illustrated, the H₂O₂-induced cytotoxic effect was considerably increased in Gpx1-under-expressing cells. After exposure to H₂O₂, the viability of BV2-under-expressing Gpx1 was less than 20 %, whereas that of the control cells was nearly 40 %.

The crucial data were the viability results of transfected cells subjected to selenite treatment in order to prevent the cell death due to oxidation. As previously described, the siRNA construct pSUPER-Gpx1-293 did not silence the Gpx1 expression, and pre-treatment with selenite of those cells could protect from H₂O₂-induced-damage.

Only in BV2 cells transfected with pSUPER-Gpx1-142 (which silences the expression of Gpx1), the supply of sodium selenite could not prevent the cell death induced by H₂O₂. The cell survival was diminished by the inability of selenium to stimulate the expression of the Gpx1 selenoprotein.

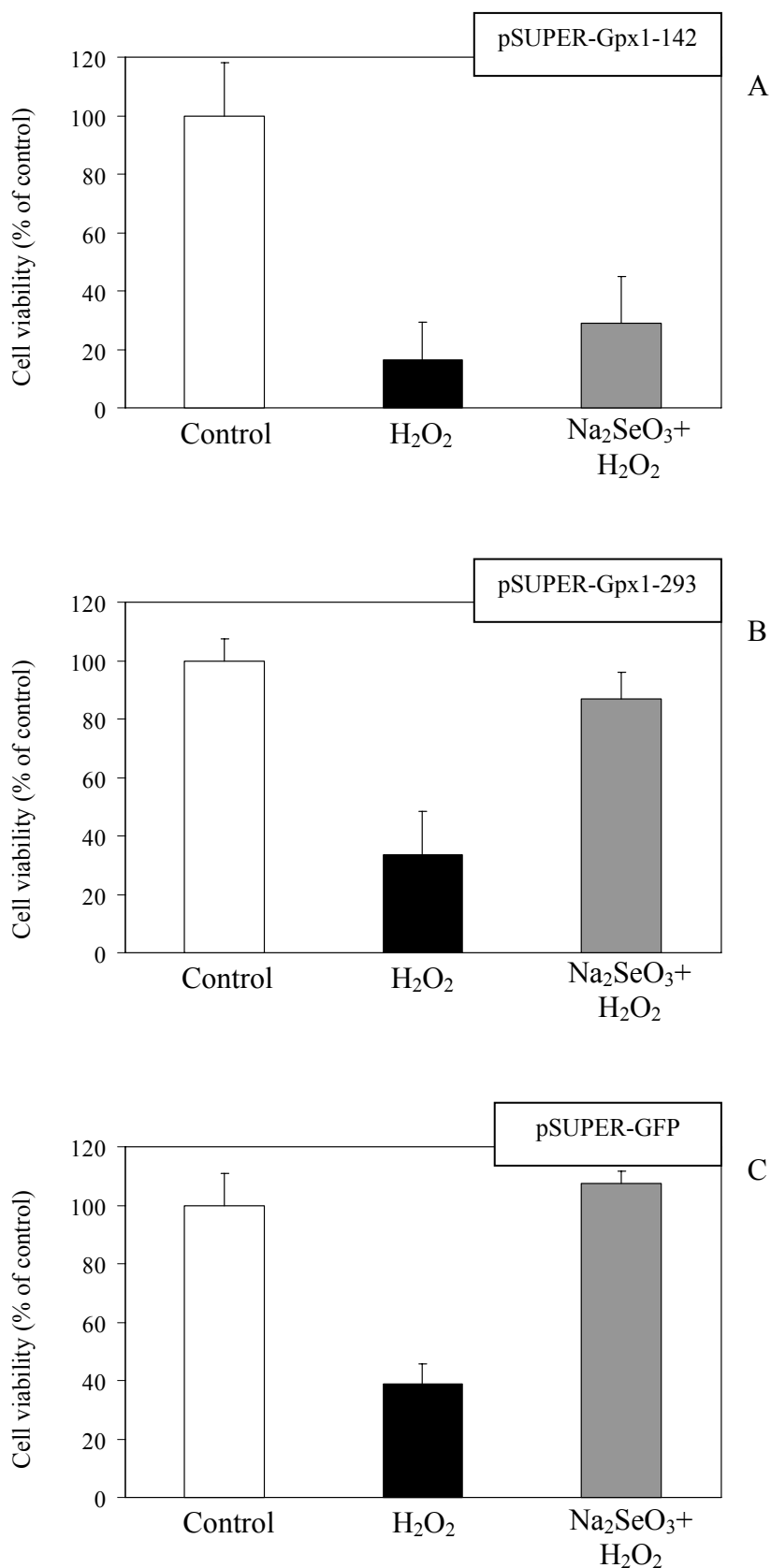


Figure 49 Effect of Gpx1 under-expression on BV2 cells exposed to oxidative stress. The cells were transfected with pSUPER-Gpx1-142 (A), pSUPER-Gpx1-293 (B) siRNA vectors and with the pSUPER-GFP empty vector as control (C) using the electroporation technique. 24 hours after transfection, sodium selenite and/or H₂O₂ were added and MTT assay was performed as described previously.

5.15.3 Subcellular localization of Gpx1

To investigate the cellular distribution of Gpx1, the generated C-terminal GFP-fusion construct (Gpx1-EGFP-C1) was transfected in COS-7 cells. The control vector (pEGFP-C1) was also transfected to compare the green fluorescence protein (GFP) distribution in the cell compartments. The GFP expression (Figure 50, above) was homogeneously distributed in the nuclei and cytosol, while Gpx1-eGFP (Figure 50, below) revealed the specific accumulation in organelles (small vesicle) in the cytoplasm and also showed a nuclear localization.

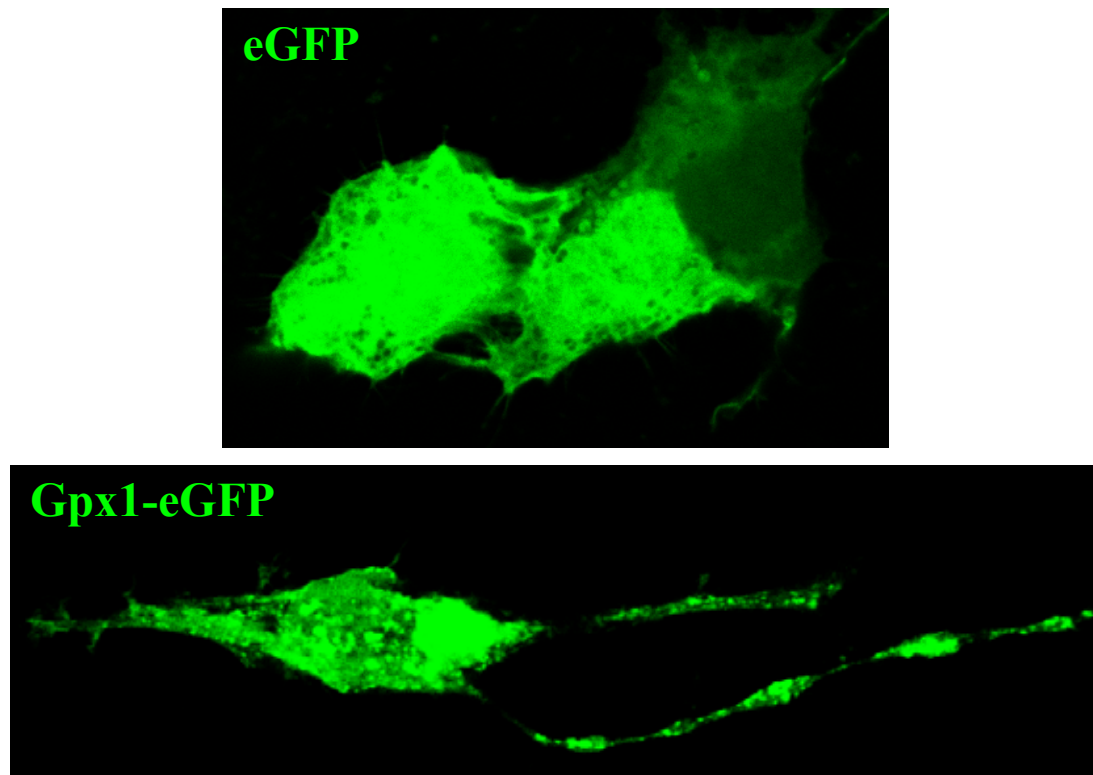


Figure 50 Localization of Gpx1. Confocal images of COS-7 cells expressing GFP-fused Gpx1 and GFP control protein 24 hours post transfection. COS-7 cells were transfected with pEGFP-C1 (upper panel) and with Gpx1-EGFP-C1 (lower panel) plasmids using the Amaxa Nucleofector electroporation method.

To further determine the subcellular distribution of Gpx1, the localization of the fusion protein was determined with a series of organelle-specific markers for endoplasmic reticulum (Calnexin), mitochondria (Prohibitin), Golgi compartment

(58K Golgi protein), Early Endosome (EEA1) and Late Endosome (Mannose 6-Phosphate Receptor). For nuclei, Hoechst staining was performed.

The recombinant plasmid (Gpx1-EGFP-C1) was transfected into COS-7 cells using the electroporation method. Cells were monitored for fluorescence between 7-24 h post transfection using fluorescence microscopy. After having fixed the cells, staining of the different organelles was applied. The transfected cells were viewed using confocal and fluorescence microscopy.

In cell transfection studies, the GFP-Gpx1 fusion protein was localized preferentially in the Golgi compartment and nuclei; it was not found to be present in ER, LE, or EEA (Figure 51 and Figure 52).

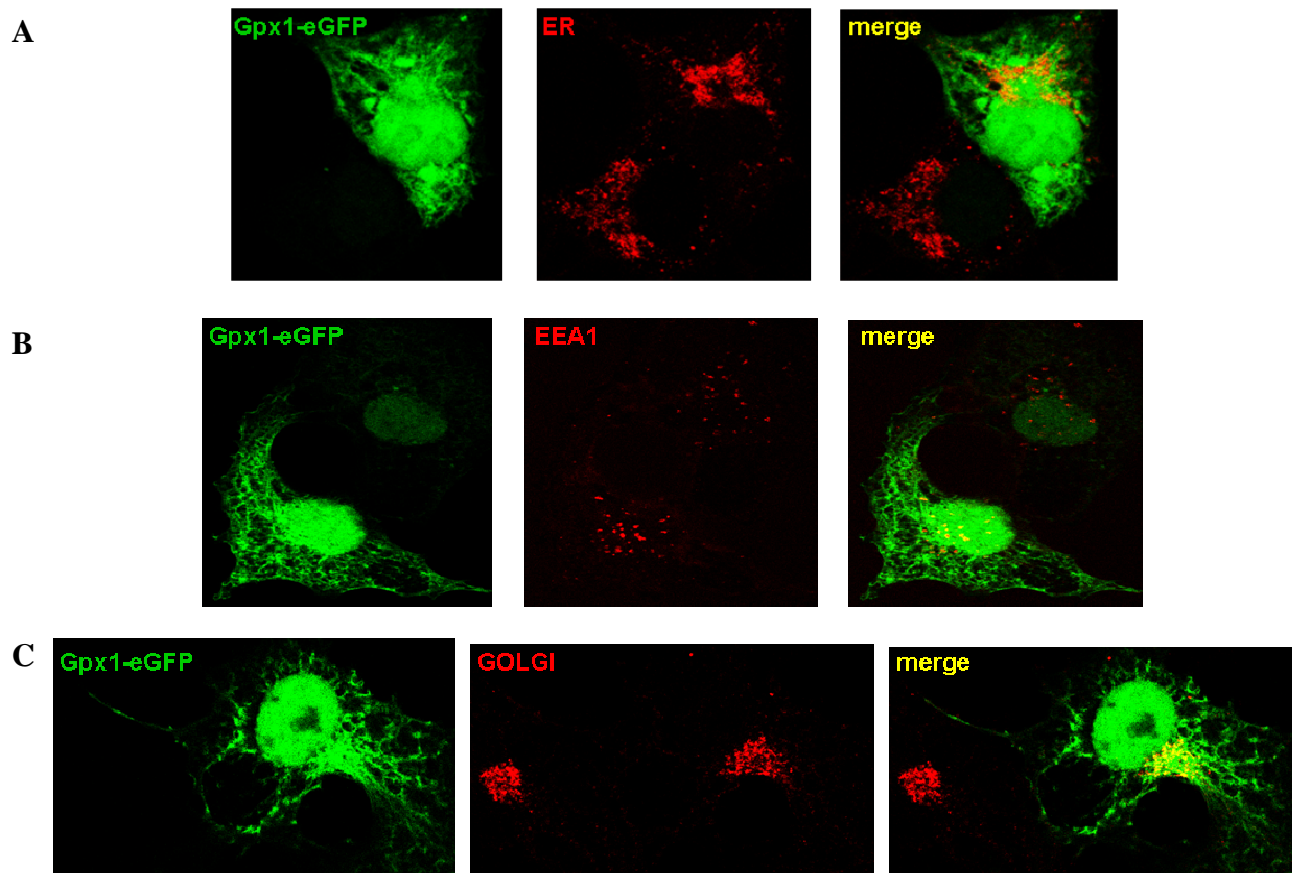


Figure 51 Confocal microscopy images of COS-7 cells transfected with DNA encoding Gpx1-eGFP (enhanced green fluorescence protein) and stained with different organelle-specific markers. The cells were imaged using confocal microscopy 24 h following transfection and stained with specific markers. Green images represent the expression of Gpx1 and red images represent different organelles. Merged colour image: superimposed image of green and red. Cells were transfected with Gpx1-EGFP-C1 and stained with: A) Calnexin, ER marker. B) EEA1, for Early Endosome. C) 58K Golgi protein, Golgi marker.

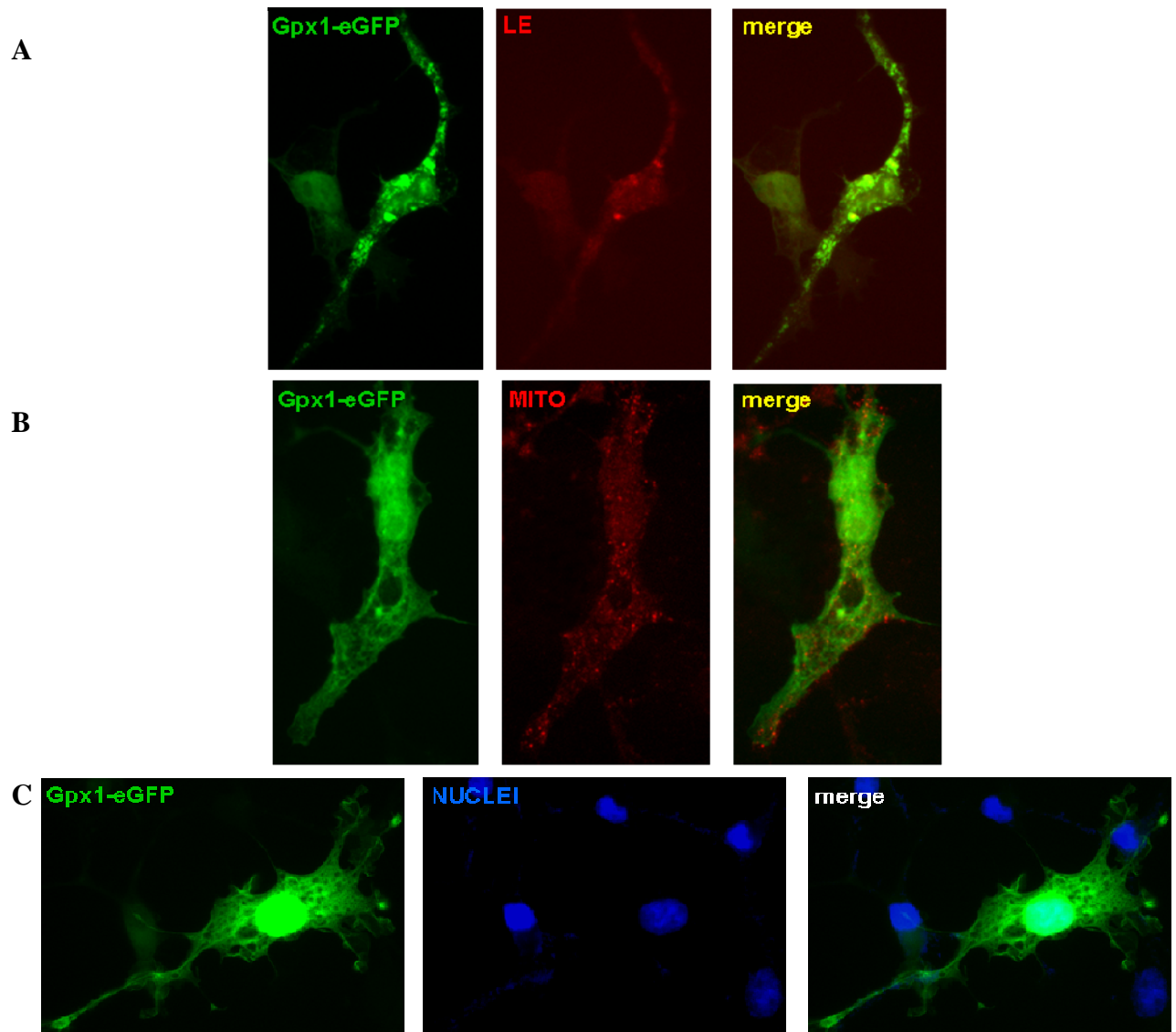


Figure 52 Fluorescence microscopy images of COS-7 cells: transfection and imaging were performed in the same manner as described in Figure 51. A) Mannose 6-Phosphate Receptor, Late Endosome marker. B) Prohibitin, mitochondria marker. C) Hoechst staining, nuclei.

5.16 Studies on primary cell cultures



Figure 53 Pictures of new born rats. Left: P1 rats deriving from animals fed a selenium-deficient diet. Right: P2 rats from animals fed a selenium-sufficient diet. The rats showed no phenotype differences.

To confirm the results obtained *in vitro* on BV2 cells, experiments on primary microglia cells were carried out. Primary microglia cells were isolated from new-born rats deriving from animals fed a selenium-deficient and selenium-sufficient diet for several generations. The aim of this investigation was to investigate if the selenium-sufficient microglia were more resistant to oxidative damage than the selenium-deficient cells. Primary cells were prepared as described and the microglia-enriched fraction was counted and seeded at the density of 4000-6000 cells/ well into 96-well culture dishes. After adhering overnight, the primary cells were either left untreated (control) or were treated with H_2O_2 . After 4 hours the induced cell death was measured by propidium iodide (PI) staining and the ROS production was also assayed as described in the method section. The production of ROS by the microglia (obtained from selenium-sufficient and selenium-deficient rats) after H_2O_2 treatment is shown in Figure 54. The ROS production in Se-sufficient microglia was increased by a factor of about ~ 1.5 compared with the untreated cells. In contrast, the selenium-deficient microglia were much more sensitive to the hydrogen peroxide treatment and produced about 4 times more ROS than the control cells.

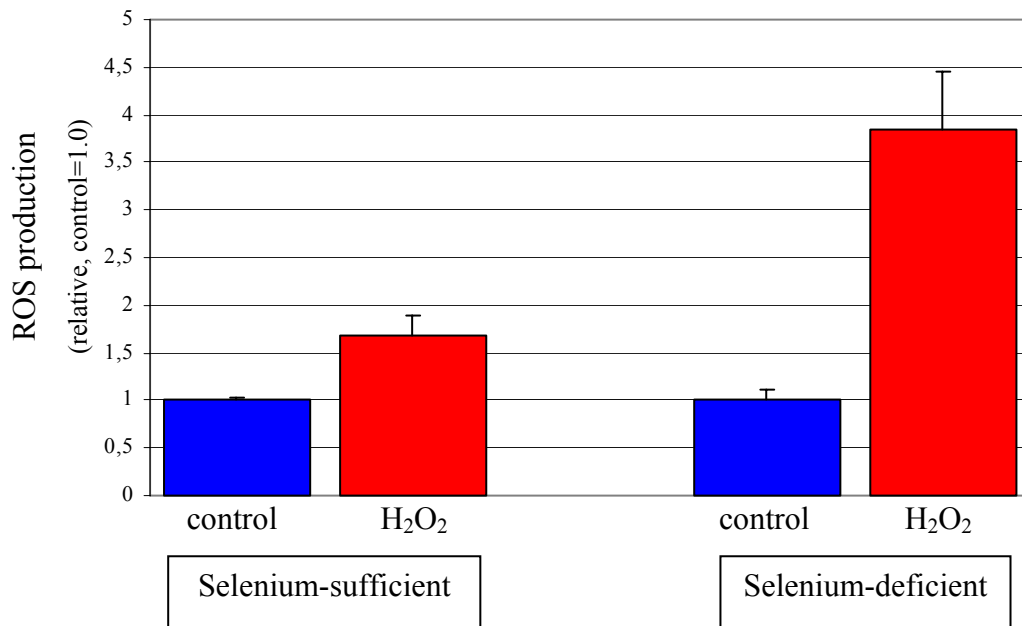


Figure 54 ROS production by primary microglia cells isolated from rats fed a selenium-sufficient or a selenium-deficient diet. Isolated microglia cells were plated on 96-well dishes, treated with H₂O₂ (250 μ M for 4 hours) and assayed for ROS production. Data are expressed in relation to untreated cells (control, 1.0).

Propidium iodide staining was applied to the same primary cell cultures to detect cell death. As shown by propidium iodide staining in Figure 55, the incubation of primary microglial cells (selenium-sufficient) with H₂O₂ caused little or no cell death (Figure 55 – A). In contrast, there were significantly more PI-positive microglial cells in selenium deficiency condition. Significantly more microglia died in cultures derived from selenium-deficient rats than in those derived from selenium-sufficient rats. Thus, these data demonstrate an enhanced susceptibility of microglia from selenium-deficient rats to an oxidative stressor such as H₂O₂.

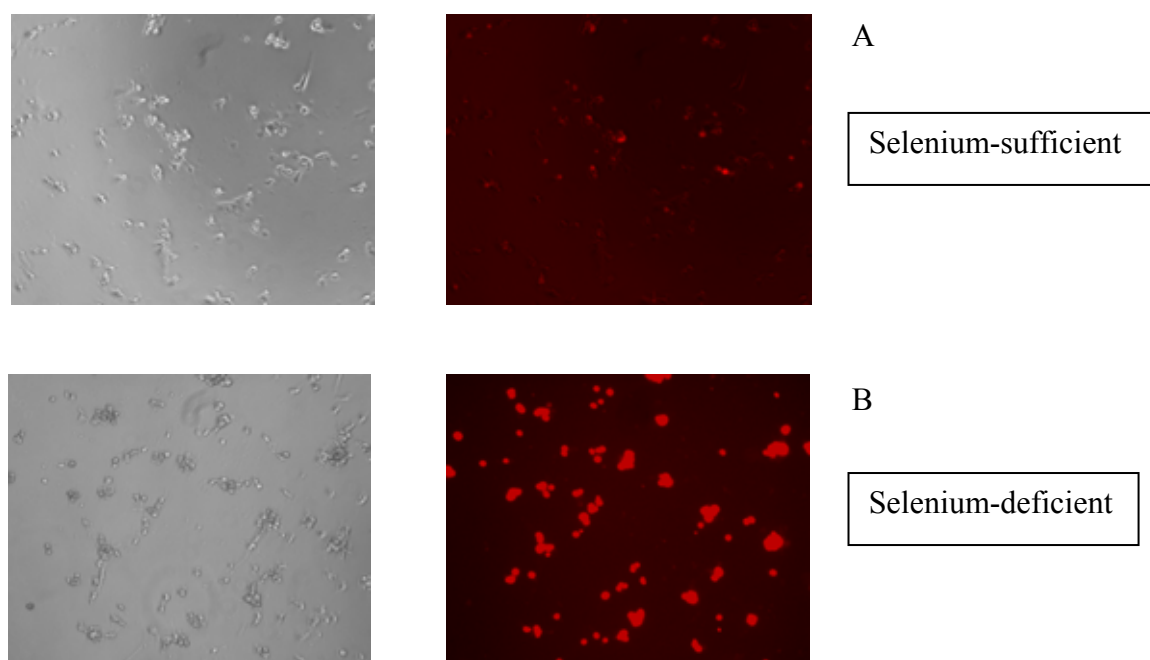


Figure 55 Bright-field (left) and rhodamine-fluorescence (right) micrographs of primary microglial cells from selenium-sufficient (A) and selenium-deficient (B) rats after H_2O_2 treatment. PI-positive (red) cells indicate cell death. Cell death was visualized with PI staining (5 $\mu\text{g}/\text{ml}$, incubated for 5 min).